ACS APPLIED MATERIALS & INTERFACES

www.acsami.org

Research Article

MXene Composite Electromagnetic Shielding Materials: The Latest Research Status

Yi Liu, Yuanjun Liu,* and Xiaoming Zhao

Cite This: https://doi.org/10.1021/acsami.4c11189

Read Online

ACCESS | Metrics & More | Article Recommendations

ABSTRACT: MXene emerges as a premier candidate for electromagnetic shielding owing to its unique properties as a novel two-dimensional material. Its exceptional electrical conductivity, chemical reactivity, surface tunability, and facile processing render it highly suitable for diverse electromagnetic shielding applications. The research status of MXene and MXene-based electromagnetic shielding materials is systematically discussed in this paper. First, the research status of MXene as a single-component electromagnetic shielding material is briefly introduced. Subsequently, the research status of composite structures constructed by MXene with polymers, carbon derivatives, and ferrites is introduced in detail. Furthermore, the research progress of MXene-based ternary and quaternary composite electromagnetic shielding materials is further focused. Finally, the application of MXene-based composite electromagnetic shielding materials is prospected. A deeper understanding of MXene's electromagnetic shielding properties is facilitated by this paper, providing the direction for the future development of two-dimensional materials in the design and processing of electromagnetic shielding materials.

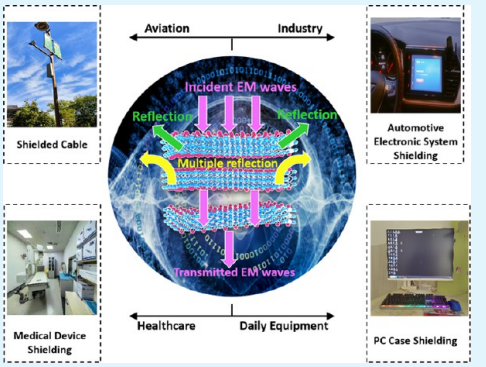

KEYWORDS: *electromagnetic shielding, MXene, composite material, 2D material, electrical conductivity*

1. INTRODUCTION

Electromagnetic radiation, a prevalent physical phenomenon in many natural occurrences and artificial devices, is widely encountered. For example, visible light emitted by the sun constitutes one form of electromagnetic radiation. At the same time, devices such as wireless radios, television signals, microwave ovens, mobile phones, and radars generate and utilize electromagnetic radiation. High-frequency electromagnetic radiation may cause interference with electronic devices, affecting their durability and operational efficiency. Additionally, electromagnetic radiation emitted by electronic devices can impact animal navigation.[1] Furthermore, electromagnetic radiation may affect human health, potentially influencing the physiological and nervous systems and leading to symptoms such as sleep disturbances, headaches, and lack of concentration. Hence, electromagnetic shielding materials are crucial in today's technological advancements and engineering applications. They are significant for safeguarding equipment, maintaining human health, ensuring information security, and developing novel technologies. The role of electromagnetic shielding materials is achieved through their internal structure and composition, utilizing physical processes such as absorption, reflection, and scattering to reduce the propagation and penetration of electromagnetic radiation.[2] The total attenuation of electromagnetic waves, known as the shielding effectiveness (SE_T), is determined by the attenuation caused by absorption (SE_A), reflection (SE_R), and multiple reflections (SE_M).[3] The magnitude of the SE_T value is closely associated with the effectiveness of the shielding material. When SE_T is less than 10 dB, it indicates no shielding effect; when SE_T falls within the range of 10−30 dB, it signifies minimal effective shielding; and when SE_T is greater than or equal to 30 dB, it represents optimal efficiency for industrial application shielding materials.[4] Additionally, the effectiveness of shielding materials can also be observed through parameters such as shielding efficiency (SE), absolute shielding efficiency per unit thickness (SSE/t), specific shielding efficiency (SSE/ρ), and conductivity (σ).[5] Shielding effectiveness (SE) is a direct indicator of the material's shielding effect on electromagnetic waves, usually measured in decibels (dB), representing the degree of intensity reduction of electromagnetic waves after passing through the shielding material.[6] The higher the SE value, the better the shielding effect of the material. The absolute shielding effectiveness per unit thickness (SSE/t) is the ratio of shielding effectiveness to material thickness used to measure the

Received: July 6, 2024
Revised: July 19, 2024
Accepted: July 19, 2024

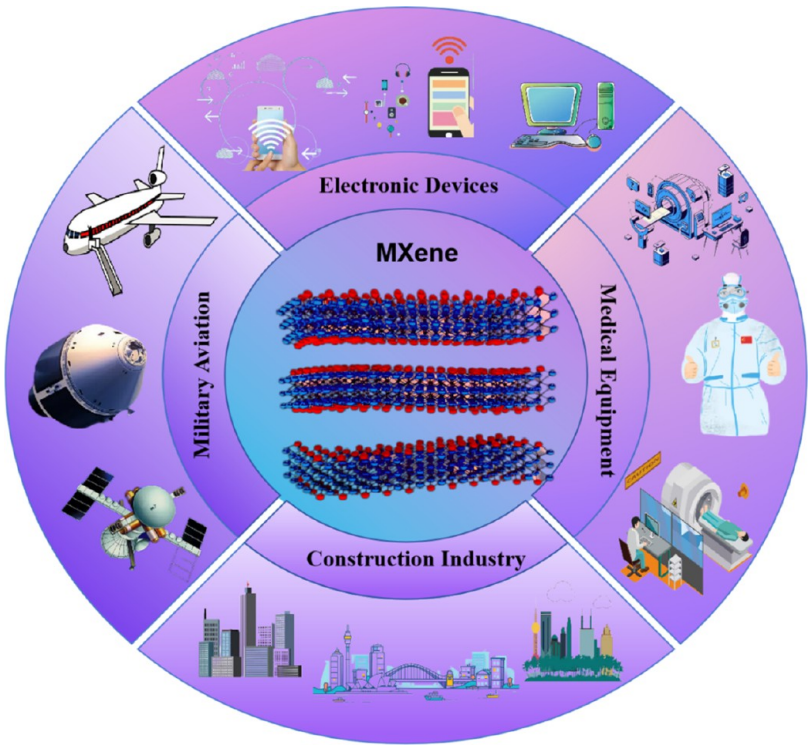

Figure 1. Structure and application of MXene.

shielding effect of the material per unit thickness.[7] The higher the SSE/t value, the better the shielding effect the material can provide even when thin, which is important for applications that require lightweight or space-limited scenarios. The specific shielding effectiveness (SSE/ρ) refers to the shielding effectiveness per unit density, that is, the ratio of the material's shielding effect to its density. The higher the SSE/ρ value, the better the shielding performance the material has under the same mass, which is very valuable for applications that need to reduce weight. In addition, conductivity (σ) is an essential indicator for measuring the material's ability to reflect electromagnetic waves, usually expressed in Siemens per meter (S/m). Materials with high conductivity can effectively hinder the propagation of electromagnetic waves, converting their energy into heat energy, thereby reducing the penetration of electromagnetic waves. Overall, these parameters work together to determine the comprehensive performance of the material in electromagnetic shielding. High SE and SSE/t values indicate that the material can provide excellent shielding effects even under thin conditions; high SSE/ρ values show their advantages in lightweight design; and high σ values enhance the material's reflective ability, improving the overall shielding effect.

Electromagnetic shielding materials typically block electromagnetic wave propagation by either reflecting incident electromagnetic waves or absorbing the electromagnetic wave energy entering the material and converting it into heat, gradually dissipating energy and reducing the penetration rate of electromagnetic waves. However, conventional electromagnetic shielding materials primarily rely on reflecting electromagnetic waves, leading to the propagation of a large amount of reflected electromagnetic waves in space, which may continue to interfere with unshielded devices, resulting in secondary electromagnetic wave pollution.[8] Despite the extensive application of traditional metal materials in the field of electromagnetic shielding, they have some inherent limitations. For instance, their considerable weight and volume restrict the lightweight design in portable or wearable devices; their high rigidity makes them difficult to bend or shape, which is not conducive to achieving flexible or customized shielding solutions; the difficulty in processing increases manufacturing costs and time; they are susceptible to corrosion, which reduces shielding effectiveness and may cause secondary pollution; impedance matching issues lead to increased reflection of electromagnetic waves, affecting the shielding effect; high surface reflection rates increase the possibility of secondary reflection; they have single functions, mainly providing shielding effects without other additional functions; and poor environmental adaptability, which can lead to performance degradation under extreme conditions. Some traditional materials may perform well within specific frequency ranges but exhibit poor shielding performance at other frequencies. This leads to the so-called "multifrequency shielding problem," which necessitates effective shielding performance at different frequencies. MXene demonstrates significant advantages in electromagnetic shielding compared to other materials, primarily due to its unique physicochemical properties.[9] First, the high electrical conductivity of MXene is one of its essential characteristics, which effectively conducts the energy of electromagnetic waves, reducing their propagation. Second, MXene exhibits excellent thermal stability, allowing it to maintain performance in high-temperature environments and making it suitable for applications under extreme temperature conditions. Additionally, MXene is easy to process and can be made into thin films, coatings, and other forms, facilitating integration into various products. The surface chemistry of MXene is tunable, and its electromagnetic shielding performance can be further optimized through methods such as oxidation, doping, heat treatment, and grafting.[2] Moreover, the layered structure of MXene

https://doi.org/10.1021/acsami.4c11189
ACS Appl. Mater. Interfaces XXXX, XXX, XXX−XXX

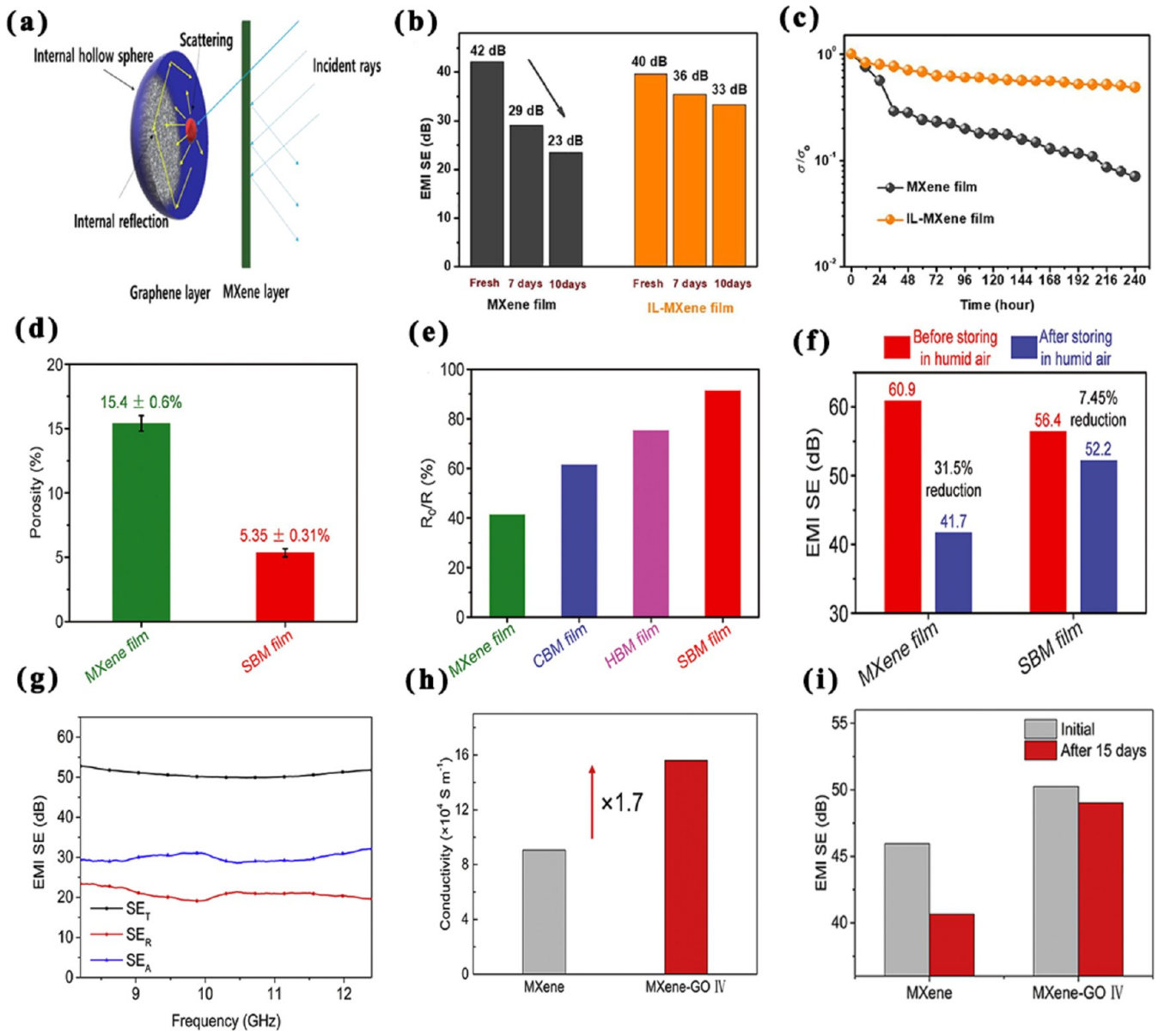

Figure 2. (a) Basic mechanism in MGNC. Reproduced with permission from ref 22. Copyright 2018 Materials (Basel). (b) SE changes and (c) normalized conductivity changes over time for MXene and IL-MXene films. Reproduced with permission from ref 25. Copyright 2020 Elsevier. (d) Porosities of MXene and SBM films derived from density measurements. (e) Conductivity retention percentages of MXene, CBM, HBM, and SBM films after repeated 360° folding for 100 cycles. (f) Average EMI SE between 0.3 and 18 GHz for MXene and SBM films before and after storage for 10 days in humid air. Reproduced with permission from ref 26. Copyright 2021 Science. (g) SE_T, SE_A, and SE_R of MXene-GO IV film. (h) Electrical conductivities of MXene film and MXene-GO IV film. (i) EMI SE changes over 15 days for MXene film and MXene-GO IV film.[27] Reproduced with permission from ref 27. Copyright 2020 American Chemical Society.

contributes to the multiple reflection and absorption of electromagnetic waves, enhancing the shielding efficiency. The controllability of this structure makes it possible to design materials with different shielding effects. MXene is also compatible with various materials[10] and can combine with polymers, carbon derivatives, nanoferrites, and metal−organic frameworks to form composite materials, further improving electromagnetic shielding efficiency. Lastly, MXene materials typically have a low density and good flexibility, making them suitable for applications requiring lightweight and flexible shielding materials. With its multifaceted advantages, MXene has become an important research direction in electromagnetic shielding materials.

MXene, a novel class of two-dimensional materials, derives its name from its structure, first discovered by Prof. Yury Gogotsi and colleagues in 2011.[11] The typical chemical formula of MXene is $M_{n+1}X_nT_x$, where M represents transition metals (usually titanium, niobium, tantalum, etc.), X represents elements such as carbon and nitrogen, *n* represents the number of layers, and *T* represents surface functional group.[12] The structure and application are shown in Figure 1. In recent years, MXene, as a type of transition metal carbide, has garnered significant attention due to its outstanding properties, including excellent conductivity, low density, high surface activity, and ease of processing.[13] The choice of MXene as an electromagnetic shielding material has its unique reasons. First, MXene's conductivity far surpasses many traditional electro-

https://doi.org/10.1021/acsami.4c11189
ACS Appl. Mater. Interfaces XXXX, XXX, XXX−XXX

magnetic shielding materials. The presence of metallic layers and the multilayer structure provide high electron mobility, rendering it an excellent conductor.[14,15] Second, MXene is a two-dimensional multilayer material in which the metal layer is composed of transition metal elements, and the layer formed by elements such as carbon and nitrogen is in between the metal layers.[16−18] This two-dimensional structure allows MXene to capture and scatter electromagnetic waves efficiently. In contrast, traditional three-dimensional shielding materials perform poorly in this respect.[19] Third, the surface of MXene contains many functional groups, making it easy to modify or compound the surface to reduce the surface conductivity, achieve good impedance matching, and reduce the reflection of electromagnetic waves on its surface.[20] The surface of MXene can also be modulated by introducing different functional groups. Such surface functionalization enables precise adjustment of MXene's hydrophilicity, chemical reactivity, and other properties to suit specific electromagnetic shielding environments. Finally, MXene not only has a high specific surface area, which makes it better able to interact with electromagnetic waves, but this high specific surface area also helps to improve the absorption capacity of electromagnetic waves; MXene also has strong adsorption capacity for various molecules and ions, making it a potential application in the field of adsorption and energy storage. MXene effectively shields electromagnetic radiation across a wide frequency range, addressing the "multifrequency shielding problem," thus endowing it with potential electromagnetic shielding performance in various application scenarios. The choice of MXene as an electromagnetic shielding material can be combined with other components to synergistically utilize the advantages of each component, further enhancing the electromagnetic shielding, conductivity, and mechanical properties of composite materials, thereby expanding their applications in the field of electromagnetic shielding. With the increasing application of MXene in the electromagnetic shielding field, it is necessary to conduct systematic and timely research on developing MXene and MXene-based composites in the electromagnetic shielding field.

In summary, this paper discusses the excellent performance and research status of MXene and MXene-based multielement composites in electromagnetic shielding. First, the current research status and progress of MXene as a monolithic electromagnetic shielding material are briefly introduced. Subsequently, the binary composite structure of MXene with polymers, ferrites, and carbon derivatives is introduced in detail, and the novel properties and application prospects of MXene-based ternary composite electromagnetic shielding materials are further analyzed. Moreover, the research progress on MXene-based quaternary composite electromagnetic shielding materials is discussed. Finally, the development direction of MXene-based composite electromagnetic shielding materials is outlined, highlighting the current research shortcomings and challenges while proposing key areas and directions for future investigation. This paper endeavors to provide a fresh perspective on understanding the role of MXene in the field of electromagnetic shielding mechanisms, laying a theoretical foundation for the design and synthesis of high-performance electromagnetic shielding materials. Additionally, it offers valuable insights for researchers engaged in various fields such as electronic communication and information technology, defense technology, electronic equipment manufacturing, aerospace, and other related domains.

2. MXENE UNITARY ELECTROMAGNETIC SHIELDING MATERIAL

MXene, as an EMI shielding material, is characterized by its significant potential, wideband response, high absorption rate, lightweight nature, tunability, high conductivity, and corrosion resistance, all of which contribute to its outstanding performance in electromagnetic shielding. MXene's layered structure is similar to graphene, which helps to improve the efficiency of electromagnetic wave absorption. The multilayered stacking structure provides MXene with a larger surface area, increasing the absorption path of electromagnetic waves and enhancing its performance. Shahzad et al. reported an MXene film with a thickness of 45 μm exhibiting an EMI shielding effectiveness of 92 dB, the highest among synthesized materials of similar thickness to date.[21] This performance was attributed to the higher electrical conductivity of the MXene film and the multiple internal reflections within the MXene layers in the film. Raagulan et al. prepared MXene and graphene-based foams (MGNC) using cost-effective spraying and solvent-casting methods.[22] The EMI shielding of the MGNC is illustrated in Figure 2a. The material demonstrated an electrical conductivity of 13.68 $S{\cdot}cm^{-1}$ and a minimum thin-layer resistance of 3.1 $\Omega{\cdot}sq^{-1}$. Within the frequency range of 8−12.4 GHz, the shielding effectiveness of MXene-graphene foam reached 53.8 dB, with a reflection coefficient of 13.10 dB and an absorption rate of 43.38 dB, showcasing exceptional electromagnetic shielding performance. The absolute shielding effectiveness of a single-layer carbon fabric reached as high as 35369.82 $dB{\cdot}cm^2{\cdot}g^{-1}$. Liu et al. fabricated MXene foam by assembling MXene flakes into a film followed by a benzene hydrazide-induced foaming process.[23] The MXene foam achieved an electromagnetic shielding effectiveness of approximately 70 dB, primarily due to its well-defined porous structure, enabling efficient absorption of electromagnetic waves. Yun et al. systematically explored the electromagnetic shielding performance of MXene-assembled films across a range of single to multiple-layer film thicknesses, employing theoretical models to elucidate the shielding mechanisms below skin depth.[24] Under this mechanism, multiple reflections became apparent, and surface reflections and significant absorption of electromagnetic radiation also occurred. While a single-layer assembled film provided around 20% electromagnetic wave shielding performance, a 24-layer film with a thickness of approximately 55 nm achieved 99% shielding effectiveness, with an absolute shielding efficiency of 3.89 × 106 $dB{\cdot}cm^2{\cdot}g^{-1}$, underscoring MXene as the optimal choice for lightweight EMI shielding applications.

Due to its dielectric loss, MXene exhibits microwave absorption characteristics; however, pure MXene lacks magnetic loss capability, resulting in mismatched impedance and inferior microwave absorption performance. Xu et al. used radiofrequency N_2 plasma to process MXene for nitrogen modification.[28] The results showed that the electromagnetic wave absorption performance of the nitrogen-doped MXene layer was significantly enhanced. The primary mechanism combined dielectric loss, magnetic loss, and suitable impedance matching in nitrogen-doped MXene. In this context, the magnetic loss mechanism of nitrogen-doped MXene is mainly due to the incorporation of nitrogen atoms, which alters the electronic structure of MXene and increases its magnetic permeability. Additionally, lattice distortion occurs, subsequently affecting the movement of magnetic domain

https://doi.org/10.1021/acsami.4c11189
ACS Appl. Mater. Interfaces XXXX, XXX, XXX−XXX

walls, leading to increased magnetic losses. A significant challenge encountered in the practical application of MXene is its susceptibility to oxidation in humid or aqueous environments. This leads to the disintegration of its two-dimensional layered structure within just a few days. Wan et al. treated easily oxidized MXene with imidazolyl ionic liquid, effectively improving the chemical stability of MXene in water.[25] The impact of imidazole-based ionic liquid-treated and untreated MXene films on EMI shielding performance and electrical conductivity was studied in high-temperature, high-humidity conditions (85 °C and 85% RH), with variations over time in shielding effectiveness and conductivity depicted in Figure 2b−2c. The shielding effectiveness of the 4.3 μm thick MXene film in the X-band and Ku-band was approximately 42 dB. Upon storage for over 5 months, the electrical conductivity and shielding effectiveness of the imidazole-based ionic liquid-treated MXene film decreased to 1.29 × 104 $S{\cdot}m^{-1}$ and approximately 26 dB, respectively. Nonetheless, this still met the requirements for commercial applications (with an electromagnetic shielding effectiveness of roughly 20 dB), demonstrating the effective inhibition of MXene oxidation by imidazole-based ionic liquids. Ying et al. achieved surface charge polarization of wrinkled MXene through chemical etching, where the wrinkles were caused by tiny creases resulting from abundant Ti vacancies under chemical etching.[29] When the MXene thickness was 20 μm, the shielding effectiveness reached 107 dB. The enhancement in EMI shielding originated from the resonant absorption of dipole moments caused by the asymmetric charge density distribution near Ti defects.

The electromagnetic shielding property of MXene film can be weakened due to the effect of the void in its structure. Wan et al. used the sequential bridging method of hydrogen and covalent bonding agents to promote the densification of MXene films and eliminate the gaps in the structure (Figure 2d) and prepared three kinds of hydrogen-bonded MXene films with different sodium carboxymethyl cellulose content, namely HBM, CBM, and SBM films.[26] Insulating carboxymethyl cellulose sodium molecules into the MXene interlayers improved film orientation and reduced crystal plane spacing. They resulted in the 3.0 μm-thick SBM film exhibiting higher conductivity within the 0.3−18 GHz range. Consequently, its EMI shielding effectiveness reached up to 56.4 dB. Moreover, even after 10 days of storage in humid air, the SBM film showed minimal degradation in its shielding performance (Figure 2e−2f). Excellent electrical conductivity enables high EMI shielding efficiency for HBM, CBM, and SBM films, whose primary shielding mechanism is absorption, partly due to their layered structure. On the one hand, densification makes the MXene film's internal structure more compact, increasing the contact area between the electromagnetic waves and the material, and enhancing the absorption efficiency.[30] On the other hand, the dense MXene film reduces the internal voids, thereby decreasing the scattering and reflection of electromagnetic waves within the material, leading to more electromagnetic energy being absorbed by the material. By spray-drying coating, Zhang et al. adhered MXene evenly and tightly to the preformed fabric.[27] By adjusting the spray drying period, the degree of conductive interconnection of the fabric can be precisely adjusted, thus providing a highly conductive, breathable fabric with EMI shielding. The results showed that the MXene-modified fabric containing a low concentration of 6 wt % (0.78 $mg{\cdot}cm^{-2}$) exhibited an excellent electrical conductivity of 5 $\Omega{\cdot}sq^{-1}$ and had good electromagnetic shielding properties. Xia et al. promoted the densification of MXene films by using graphene oxide (GO) as a bridging agent.[31] The conductivity of MXene films increased to approximately 1.6 × 105 $S{\cdot}m^{-1}$, reaching 1.7 times that of the original MXene film. At a thickness of 10 μm, the electromagnetic shielding performance reached 5.2 × 106 $dB{\cdot}m^{-1}$, as depicted by the SE value in Figure 2g. The compact structure improved the environmental stability of the MXene film, and after 15 days, its conductivity and EMI shielding properties remained at 88.7 and 90.0%, as shown in Figure 2h−2i.

The base material of pure MXene, as an electromagnetic shielding material, possesses a unique two-dimensional layered structure, multilayer stacking, and surface functional groups, endowing it with high electromagnetic wave absorption performance.[32] However, pure MXene has some limitations, such as its limited absorption efficiency at specific frequencies and the need for more performance adjustment in specific engineering applications. Consequently, the formation of composite structures by combining MXene with other materials can fully leverage each material's advantages and compensate for the deficiencies of individual materials. Composite materials can achieve a broader frequency response and higher absorption rates and adapt to the demands of various engineering scenarios through adjustments in MXene content, interaction with other components, and other means.

3. MXENE-BASED BINARY COMPOSITE ELECTROMAGNETIC SHIELDING MATERIAL

MXene has several advantages, such as excellent electromagnetic shielding performance, but it also faces challenges. MXene's mechanical strength, flexibility, and structural stability could be better, thus restricting its application in specific contexts.[33] Moreover, MXene is prone to oxidation in humid environments, decreasing electromagnetic shielding performance. Consequently, addressing the mechanical performance and stability issues of MXene and its oxidation characteristics in humid environments constitutes a key challenge for advancing MXene's development in electromagnetic shielding applications. By comprehensively considering these factors, MXene's potential in the field of electromagnetic shielding can be better realized. The electromagnetic shielding performance of MXene is closely related to its structure and chemical properties, and the limitations mainly involve frequency dependence, processing conditions, material thickness, and stability. To further enhance MXene's electromagnetic shielding performance, it can be combined with other materials to create various composite materials, such as polymers, carbon derivatives, and ferrites.

3.1. MXene/Polymer. Because of its high electrical conductivity and low dielectric loss, MXene still causes strong reflection of electromagnetic waves when combined with polymers to form composites.[34] Therefore, Han et al. prepared MXene/PU composites using a vacuum-assisted filtration method.[35] The results showed that the composite material with a mass fraction of 2 wt % MXene can absorb 90% of electromagnetic waves covering the entire X-band. This research indicated a new frontier in developing thin, highly absorbent MXene-based electromagnetic protection materials. Kim et al. prepared MXene/plasticized polyurethane (MX/APU) composite foam material for electromagnetic shielding and impact absorption, and the preparation process is shown in

https://doi.org/10.1021/acsami.4c11189
ACS Appl. Mater. Interfaces XXXX, XXX, XXX−XXX

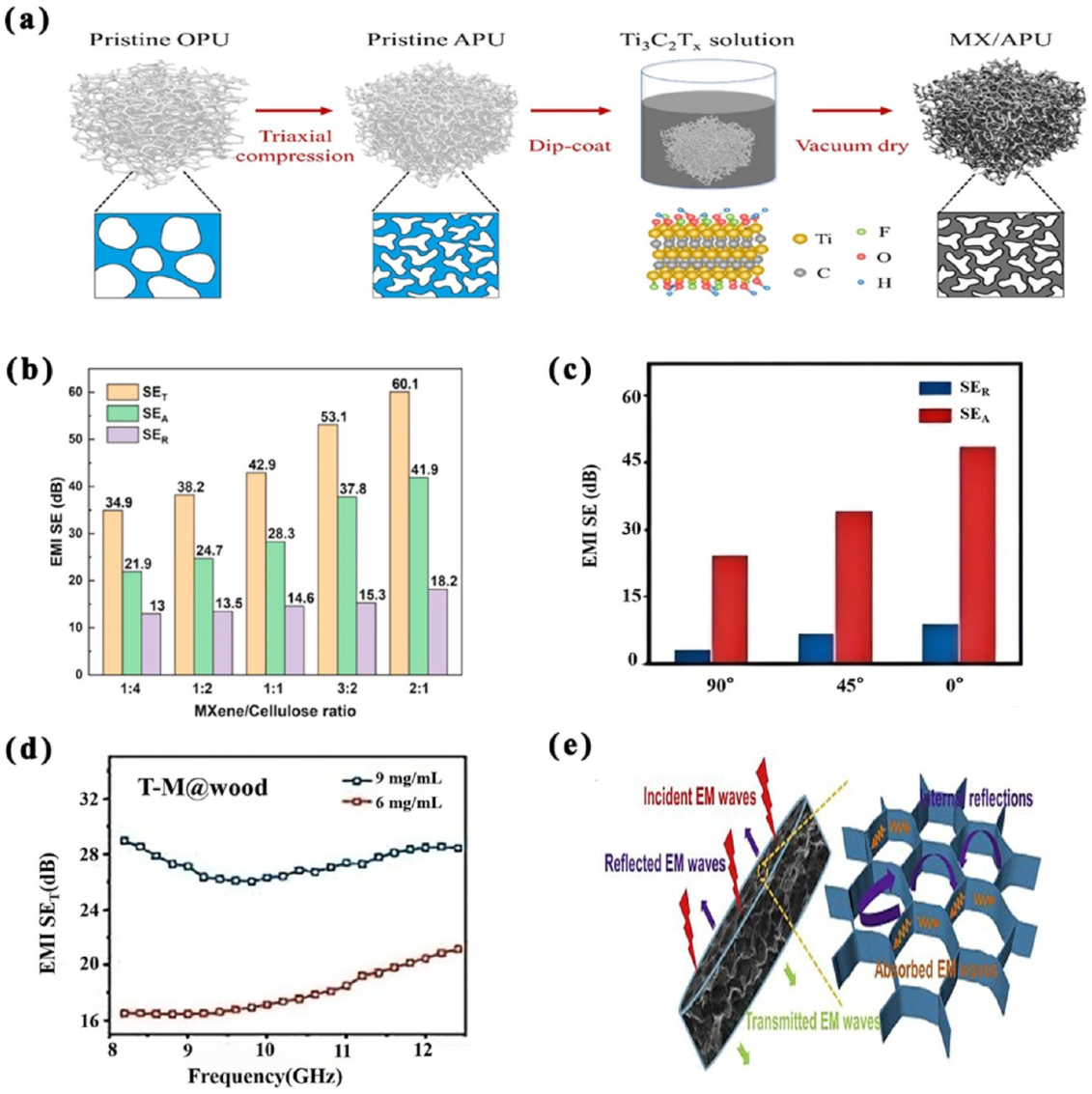

Figure 3. (a) Schematics of MX/APU composite foam fabrication. Reproduced with permission from ref 36. Copyright 2021 Elsevier. (b) average EMI shielding effectiveness. Reproduced with permission from ref 39. Copyright 2021 Elsevier. (c) SE_R, SE_A of T-M@ wood in the X-band. (d) EMI SE_T of T-M@ wood. Reproduced with permission from ref 40. Copyright 2023 Elsevier. (e) Possible EMI shielding mechanisms of the nanocomposite film by forming a continuous MXene network. Reproduced with permission from ref 41. Copyright 2019 Elsevier.

Figure 3a.[36] At the same density, the electromagnetic shielding efficiency of MX/APU composite materials reached 76.2 dB, surpassing nonexpandable counterparts by 31.2%. This enhancement was attributed to the larger surface area provided by the expandable structure. Due to its ultralow density of 0.063 g·cm^{-3}, the material produces an SE ratio of 1210 dB·cm^3·g^{-1}, making it the optimal choice for lightweight applications. The inherent conductivity, tunability, flexibility, and small thickness of MXene and MXene@ conductive polymer composites make them suitable for EMI shielding applications.[37] Zhai et al. prepared waste cotton cellulose aerogel by dissolving waste cotton fabric (WCF) and coated MXene nanosheets on the cellulose aerogel to form WCF/MXene composite aerogel.[38] The WCF/MXene composite aerogels possessed a highly porous network structure, excellent conductivity (surface resistance of 8.2 Ω·sq^{-1}), and high electromagnetic shielding efficiency within the 2−18 GHz range. Additionally, Zhu et al. prepared a tough double-layer MXene/cellulose paper with ultrahigh electrical conductivity through vacuum-assisted filtration and hot pressing.[39] By tightly assembling several layers of MXene on a cellulose substrate by hydrogen bonding, an efficient and interconnected conductive network was constructed in the paper. The highly conductive MXene layers can rapidly reflect many incoming electromagnetic waves. Thanks to the highly reflective EMI shielding mechanism, the resulting 2-layer MXene/cellulose paper exhibited excellent electromagnetic shielding with values ranging from 34.9 to 60.1 dB (Figure 3b).

Using calcium alginate (CA) and MXene as raw materials, Zhou et al. successfully fabricated a sponge-like MXene/CA aerogel film through vacuum-assisted filtration-induced self-assembly and freeze-drying methods.[42] This film, with a thickness of 26 μm, exhibited an electromagnetic shielding effect of 54.3 dB, attributed to multiple reflections and scattering enhancing the dissipation of incident electromagnetic waves. This highlights the dual benefits of combining MXene with biodegradable natural polymers for electromagnetic shielding materials—enhanced shielding effectiveness

https://doi.org/10.1021/acsami.4c11189
ACS Appl. Mater. Interfaces XXXX, XXX, XXX−XXX

and environmental sustainability, presenting a promising eco-friendly solution for addressing electromagnetic interference concerns. In addition, Wu et al. reinforced MXene nanosheets with cellulose nanocrystals (CNC) to prepare bionic composite materials with excellent electrical conductivity and electromagnetic shielding efficiency.[43] When the MXene/CNC nanocomposite was about 2−14 μm thick, the electromagnetic shielding efficiency value reached 30−66 dB, comparable to the best electromagnetic shielding effect. Additionally, Wei et al. prepared an MXene@wood composite material (M@wood) with adjustable shielding efficiency by coating MXene on the surface of natural wood. EMI SE_T of T-M@wood is shown in Figure 3d.[40] Due to its anisotropic pore structure and abundant free radicals, M@wood can sense dihedral angle change between wood grain and electromagnetic field in tangential cross-section. This enabled a switchable on/off state for electromagnetic wave transmission and shielding; when the dihedral angle changes from 90 to 0°, SE varies from 27.4 to 57.6 dB (Figure 3c). Moreover, Feng et al. produced MXene/CNF composite membranes from a multilayer MXene particles/raw cellulose fiber mixture using a vacuum filtration method, with a uniform and well-arranged structure.[44] Due to the improved structure, the conductivity and EMI shielding performance of MXene/CNF composite membrane were significantly increased by 3725.5 and 63.5%, respectively. More importantly, the electromagnetic shielding performance of the MXene/CNF composite film reached 36.51 dB at a thickness of 20 μm. Hu et al. introduced MXene nanoparticles onto the carbon fiber surface using electrophoretic deposition. hey performed thermal annealing treatment to prepare a new carbon fiber-reinforced polymer composite successfully.[45] Thermal annealing treatment reduced the number of oxygen groups on the surface of MXene nanoparticles, increased the electrical conductivity by 66%, and increased the electromagnetic shielding efficiency by 20%. The superior electromagnetic shielding performance was attributed to the uneven interface polarization, dipole polarization, and conduction loss effects induced by the annealed MXene on the carbon fiber surface. Luo et al. constructed an interconnected MXene network within a natural rubber (NR) matrix using vacuum-assisted filtration, producing a highly conductive MXene/NR nanocomposite film.[41] The electrical conductivity and electromagnetic shielding efficiency of the nanocomposite containing 6.71 vol % MXene reached 1400 $S{\cdot}m^{-1}$ and 53.6 dB, respectively, and the electromagnetic shielding mechanism is shown in Figure 3e. The negative electrostatic repulsion of MXene and NR latex enables MXene sheets to be selectively distributed at the interface of NR particles, forming an interconnected network that facilitates efficient electron transport and load transfer at low MXene content.

Xu et al. employed electrostatic self-assembly and dip-coating techniques to fabricate melamine foam (MF) composed of MXene/polydimethylsiloxane layers.[46] When the MXene packing was only 1.131 vol % in the X-band, the lightweight foam electromagnetic shielding efficiency reached 45.2 dB. Even after exposure to air for 60 days, the electromagnetic shielding effectiveness remained stable. This highlights the dual advantage of combining MXene with organic polymers, leveraging high conductivity and the flexibility of polymers to enhance overall electromagnetic shielding effectiveness. Expanding upon this, Hu et al. successfully prepared HS-MXene composite films using the MXene conductive layer and the nanofiber support layer as raw materials using step-by-step vacuum-assisted filtration and dip coating technology.[47] When the MXene mass fraction was 20 wt %, the HS-MXene composite film exhibited an electromagnetic shielding effectiveness of 46.1 dB at a thickness of 23.2 ± 0.5 μm. This was attributed to the unique layered structure, hydrogen bonding interactions, and covalent cross-linking of MXene sheets, enabling the HS-MXene composite film to demonstrate outstanding electromagnetic shielding, surpassing other reported EMI shielding materials. The composite film exhibited excellent mechanical flexibility and hydrophobicity and remained stable in electromagnetic shielding properties under cyclic bending, torsion, and humid conditions. PVA is known for its flexibility and elasticity; Yang et al. successfully prepared MXene/poly(vinyl alcohol) (PVA) biomimetic hydrogels using ice template freezing and salting-out methods. The hydrogel exhibited a honeycomb-like arrangement of porous structures.[48] Due to the synergistic interaction between MXene, PVA, water, and bionic porous structure, this thin hydrogel's EMI shielding efficiency reached 57 dB when it contained only 0.86 vol % MXene. In the ultra-wideband frequency range of 8.2−40 GHz, its electromagnetic interference shielding effectiveness exceeded 50 dB.

3.2. MXene/Carbon Derivatives. The diminished conductivity of reduced graphene oxide (rGO) foam and its singular structure result in a decreased EMI shielding performance. Chen et al. introduced highly conductive MXene nanosheets into the solution of graphene oxide (GO) and designed a multilayered structure to enhance the electromagnetic shielding performance of graphene foam.[49] The electromagnetic shielding effectiveness of the multilayered composite foam exceeded 28 dB in the C-band and 35 dB in the X-band, demonstrating outstanding EMI shielding capabilities. Tang et al. successfully fabricated a thin, flexible, and oxidation-resistant MXene-based graphene (M-rGX) porous membrane through electrostatic self-assembly and hydrogen−argon atmosphere annealing.[50] With a film thickness of 15 pm, the SSE/t reached 76422 $dB{\cdot}cm^2{\cdot}g^{-1}$, achieving optimal electromagnetic shielding. This can be attributed to the elimination of functional groups on both GO and MXene sheets, forming a porous conductive network that aids in effectively shielding incident electromagnetic waves. Furthermore, removing functional groups on MXene significantly improved the membrane's antioxidative properties, resulting in superior durability in electromagnetic shielding performance for up to 12 months. Zheng et al. employed coaxial wet spinning and freeze-drying techniques to successfully prepare reduced graphene oxide (rGO)/MXene aerogel (GMA).[51] GMA's electromagnetic shielding performance reached 83.3 dB, demonstrating excellent EMI shielding performance, significantly exceeding that of many carbon and MXene-based aerogels and foams. More importantly, due to the adequate protection of the hydrophobic graphene sheath, the electromagnetic shielding performance of GMA only decreased by 17.4% after 120 days, showing superior electromagnetic shielding durability compared with pure MXene films. These examples demonstrate the efficacy of incorporating MXene nanosheets into graphene-based structures to enhance EMI shielding performance. By leveraging the synergistic effects of MXene and graphene derivatives, such as GO or rGO, researchers have developed composite materials with improved conductivity, durability, and EMI shielding effectiveness across various applications, ranging from foam to membranes and aerogels.

https://doi.org/10.1021/acsami.4c11189
ACS Appl. Mater. Interfaces XXXX, XXX, XXX−XXX

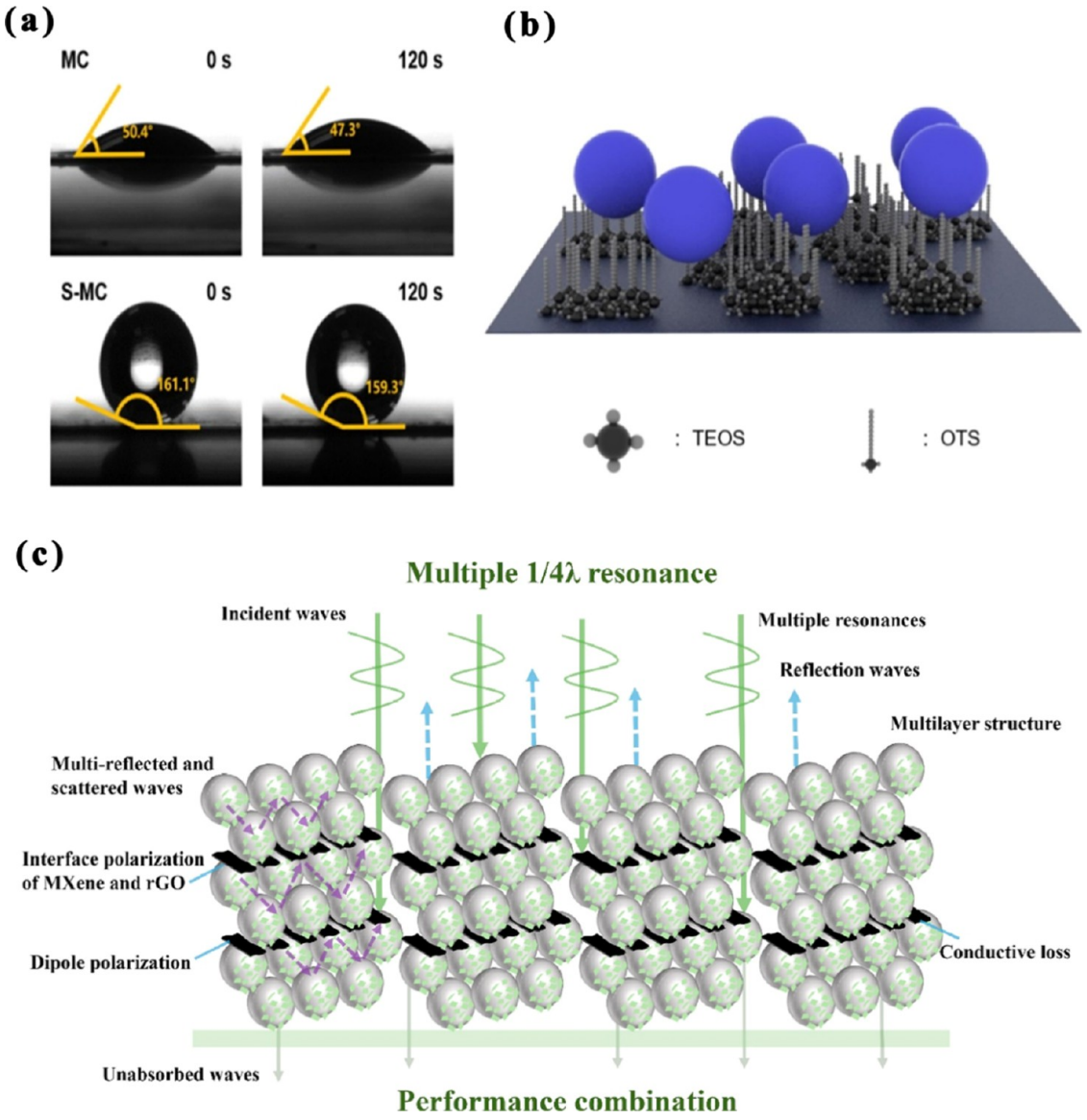

Figure 4. (a) Schematic of superhydrophobic behavior of S-MC films. (b) Contact angles of MC90 and S-MC90 composite films. Reproduced with permission from ref 52. Copyright 2023 Elsevier. (c) Scheme of absorbing and electromagnetic shielding principle of the film. Reproduced with permission from ref 53. Copyright 2022 Elsevier.

Li et al. successfully prepared a highly hydrophobic MXene/Sodium carboxymethyl cellulose (S-MC) composite film by the method of scraper coating and binary organosilane modification and compared it with the film without carboxymethyl cellulose (MC).[52] The contact angles of MC90 and S-MC90 composite films are depicted in Figure 4a−4b, showing that the S-MC film with 90% MXene content exhibited superior hydrophobic performance. The data indicated that the film's electromagnetic shielding effectiveness exceeded 30 dB. This was attributed to the synergistic effects of hydrogen bonding, arrangement of MXene nanosheets, and organic silane cross-linking, enabling the S-MC film to perform remarkably in electromagnetic shielding effectiveness. Li et al. prepared an ultrathin wideband MXene/rGO composite film (MGF) with a three-dimensional large pore structure by designing components and sandwich structure.[53] The electromagnetic shielding is shown in Figure 4c. The qualified bandwidth of this film covered the entire measurement frequency range of 0.37−2.0 THz. The maximum absorption rate of the film reached 54.2 dB, with an average absorption intensity of 43.2 dB, demonstrating electromagnetic solid shielding effectiveness. This outcome provided crucial insights for designing high-performance ultrathin broadband terahertz absorption and shielding materials. These studies provide valuable insights for developing high-performance, multifunctional MXene-based materials for hydrophobicity, electromagnetic shielding, and terahertz absorption.

3.3. MXene/Ferrite. Not only does ferrite possess high magnetism, enabling effective absorption and dispersion of electromagnetic radiation,[54] but when electromagnetic waves traverse through ferrite, the magnetic particles within it convert electromagnetic energy into thermal energy, thereby attenuating the propagation of electromagnetic waves and serving a shielding function. Additionally, ferrite exhibits favorable shielding effectiveness within a lower frequency range, making it particularly suitable for shielding against low-frequency electromagnetic radiation. MXene and ferrite function in electromagnetic wave shielding through conductivity and

https://doi.org/10.1021/acsami.4c11189
ACS Appl. Mater. Interfaces XXXX, XXX, XXX−XXX

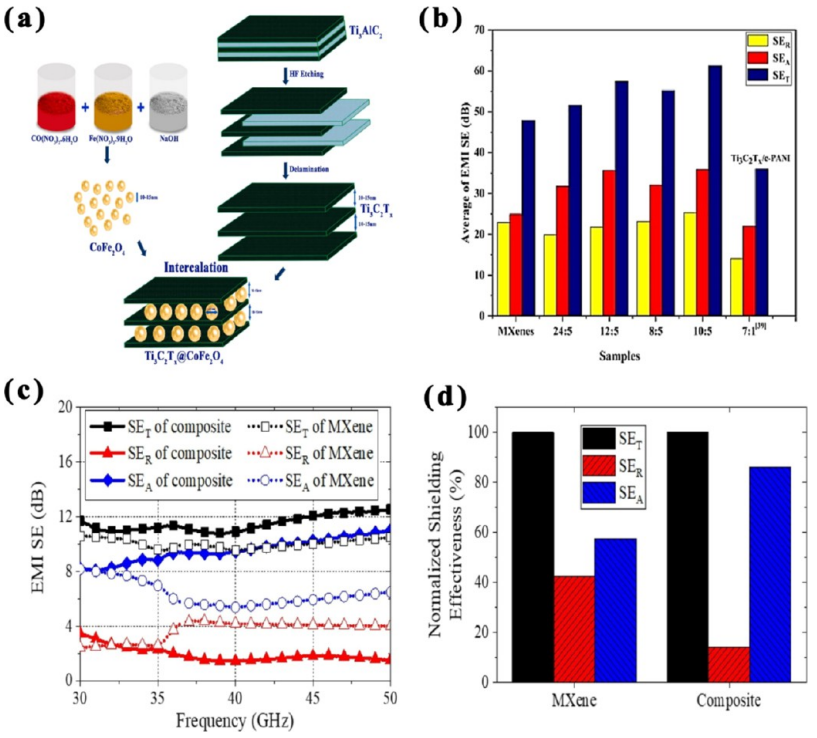

Figure 5. (a) The intercalation process of sandwich-like $Ti_3C_2T_x$@$CoFe_2O_4$ structure. Reproduced with permission from ref 56. Copyright 2022 Elsevier. (b) Average EMI SE of films with different weight ratios. Reproduced with permission from ref 58. Copyright 2020 Elsevier. (c) Shielding effectiveness of 1.5 mm thick MXene and MXene/45 wt % $BaCo_{0.3}Ti_{0.3}Fe_{11.4}O_{19}$ composite and (d) normalized shielding effectiveness of 1.5 mm thick MXene and MXene/45 wt % $BaCo_{0.3}Ti_{0.3}Fe_{11.4}O_{19}$ composite at 42 GHz. Reproduced with permission from ref 59. Copyright 2022 Elsevier.

magnetism, respectively. The different mechanisms of the two materials can complement each other to form a multilevel electromagnetic shielding effect, which improves the shielding performance of the material to different frequency electromagnetic waves. In summary, ferrite is widely used in various electromagnetic shielding applications due to its magnetic properties, frequency adaptability, stability, and cost-effectiveness, providing reliable electromagnetic protection for electronic equipment and systems.

Jin et al. obtained MXene@Fe_3O_4 magnetic nanofibers with a diameter of 25 nm by self-assembly and thermal decomposition of single-layer MXene nanosheets coated with Fe_3O_4 nanoparticles.[55] Utilizing ultrasonic atomization technology, micron-scale wrinkled porous MXene@Fe_3O_4 composite microspheres were prepared. An efficient microwave absorption system was obtained by mixing these two composite materials. This composite material's maximum adequate absorption bandwidth reached 5.2 GHz (12.8−18 GHz). The study of microwave absorption mechanism showed that due to the unique structure and impedance matching, the attenuation pathway included dielectric loss, magnetic loss, multiple reflection, and conductive loss. Swapnalin et al. synthesized MXene@$CoFe_2O_4$ composite material through hydrothermal synthesis, wherein ferromagnetic cobalt ferrite ($CoFe_2O_4$) was intercalated into two-dimensional MXene sheets, as depicted in Figure 5a.[56] When the load of $CoFe_2O_4$ was increased to a certain extent, the electromagnetic properties were enhanced, and the higher dielectric constant and permeability of the MXene@$CoFe_2O_4$ composite indicated the effective absorption of electromagnetic radiation. Mudasar et al. synthesized BCZF and V_2CT_x composite materials by integrating V_2CT_x onto the surface of BCZF with different mass ratios using the hydrothermal method and forming chemical bonds using electrostatic force.[57] The BCZF@10%V_2CT_x composite material exhibited remarkable electromagnetic wave absorption capability at an adequate absorption bandwidth of 8.0 GHz, surpassing contemporary magneto-dielectric hybrid composite materials. This superiority was attributed to the dielectric-magnetic synergistic loss mechanism induced by interface polarization, intense multiple reflections, scattering between MXene multilayer structures, conductive losses, and magnetic resonance, effectively optimizing impedance matching and enhancing the attenuation capability of the synthesized composite material.

Using MXene and Fe_3O_4@PANI composite materials as raw materials, Wang et al. prepared flexible, lightweight composite films by vacuum-assisted filtration.[58] The average EMI shielding effectiveness of films with different mass ratios is depicted in Figure 5b. The results indicated that in an ultrathin composite film with a weight ratio of MXene nanosheets to Fe_3O_4@PANI at 12:5 and a thickness of merely 12.1 μm, the maximum electromagnetic shielding effectiveness reached 58.8 dB. This was significantly higher than the electromagnetic shielding effectiveness of a pure conductive MXene film with the same thickness. By adjusting the film thickness through an increase in MXene concentration, an electromagnetic shielding effectiveness of 62 dB was achieved with a film thickness of 16.7 μm. This film exhibited excellent electromagnetic shielding performance, holding potential applications in packaging, wearable electronic devices, and military sectors. Won et al. prepared MXene/$BaCo_{0.3}Ti_{0.3}Fe_{11.4}O_{19}$ composite material by mixing MXene with ferrite particles.[59] Composites with different contents (20, 35, and 45 wt %) of $BaCo_{0.3}Ti_{0.3}Fe_{11.4}O_{19}$ were studied in the 30−50 GHz frequency range, as illustrated in Figure 5c−5d. The results showed that the average SE_T of the composite was 12 dB

https://doi.org/10.1021/acsami.4c11189
ACS Appl. Mater. Interfaces XXXX, XXX, XXX−XXX

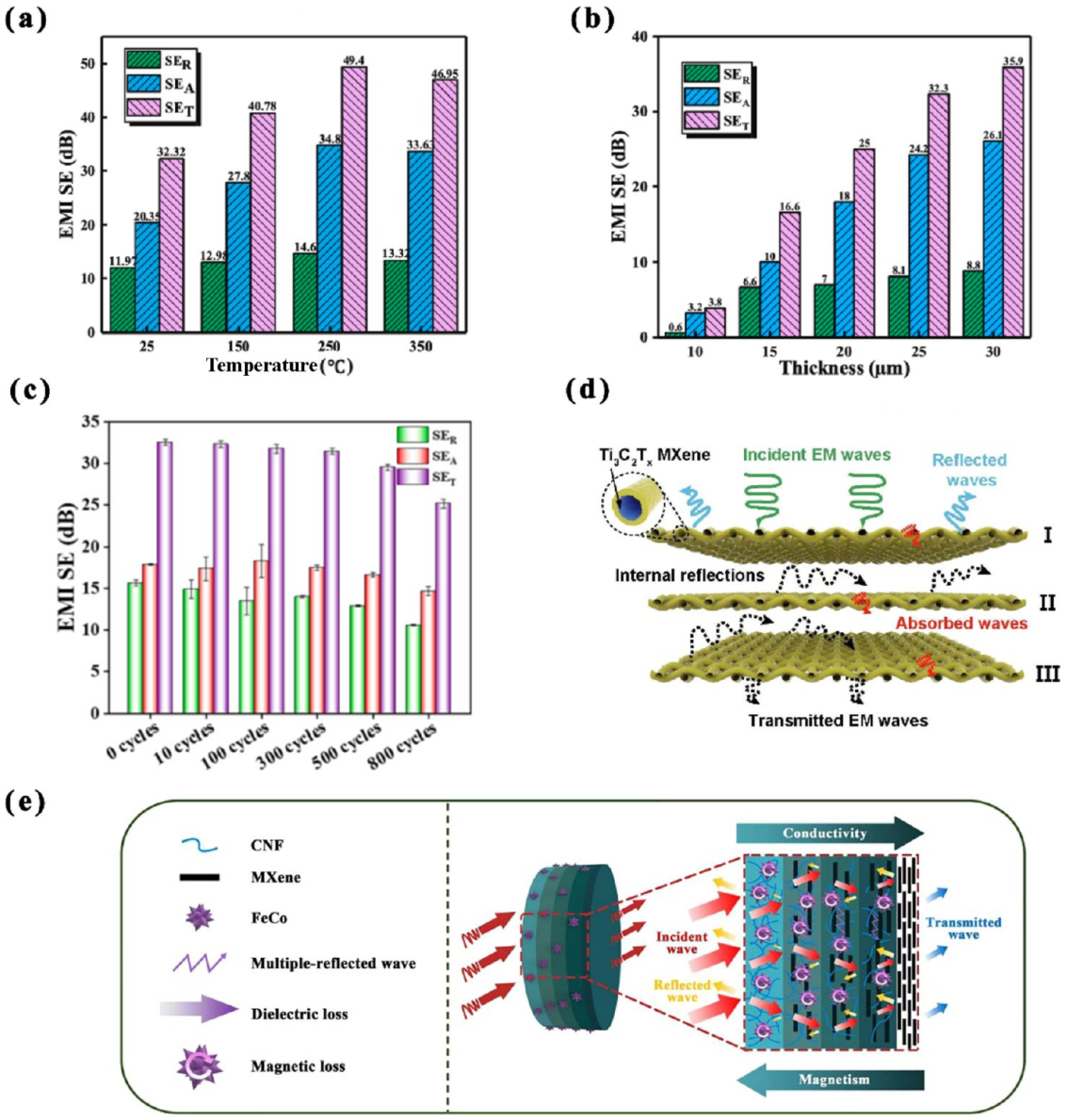

Figure 6. (a) EMI SE_T, SE_R, and SE_A of Ti_3CNT_x coatings with different thicknesses and (b) EMI SE_T, SE_R, and SE_A of Ti_3CNT_x coatings at different annealing temperatures. Reproduced with permission from ref 68. Copyright 2022 Elsevier. (c) Average SE_R, SE_A, and SE_T of 76.6 wt %-MXene/AgNWs/PEDOT: PSS coating under different bending cycles. Reproduced with permission from ref 69. Copyright 2023 Elsevier. (d) EMI shielding mechanisms of the hollow core−shell RC@M fiber textile. Reproduced with permission from ref 71. Copyright 2021 Elsevier. (e) EMI shielding mechanism of the CNF/MXene/FeCo-G composite film. Reproduced with permission from ref 72. Copyright 2022 Elsevier.

(equivalent to 94% shielding), and the composite absorbed 83.2% electromagnetic waves. The absorption performance was mainly attributed to improved impedance matching and enhancing dielectric and magnetic loss. The high magneto crystalline anisotropy of hexagonal ferrite transfers the microwave absorption peak to millimeter wave bands such as Ka- and V- bands.

4. MXENE-BASED TERNARY COMPOSITE ELECTROMAGNETIC SHIELDING MATERIAL

The layered structure of MXene, along with its abundant surface functional groups, further enhances its performance in absorbing and scattering electromagnetic waves, thereby increasing EMI shielding effectiveness. These advantages make layered MXene electromagnetic shielding materials an ideal choice, exhibiting excellent electromagnetic shielding performance and vast application potential.[60] They hold significant advantages in lightweight, efficient electromagnetic shielding and engineering processing.

Silver nanowires are extensively utilized in MXene-based composite electromagnetic shielding materials due to their excellent conductivity, good flexibility, efficient electromagnetic shielding performance, and stable chemical characteristics. A continuous conductive network can be formed by silver nanowires, effectively enhancing the conductivity of the composite material and absorbing and scattering electromagnetic waves in electromagnetic shielding, thereby improving the shielding efficiency. They exhibit good compatibility with MXene and other materials, enabling the formation of a uniform composite structure, thus enhancing the material's engineering processing performance and durability. Agglomerations occur when nanosilver wires (AgNWs) are combined

https://doi.org/10.1021/acsami.4c11189
ACS Appl. Mater. Interfaces XXXX, XXX, XXX−XXX

with MXene, which reduces the material's overall properties. To solve this problem, various strategies can be adopted. First, using surfactants effectively improves the dispersion of AgNWs and MXene by changing the interaction between particles, thereby reducing agglomeration.[61,62] In addition, the ion pre-embedding technique can expand the layer spacing of MXene, which not only helps to reduce AgNWs agglomeration with MXene but also promotes ion diffusion.[63] At the same time, cellulose nanocrystals (CNCs) can be used as stabilizers to form a stable aqueous dispersion with MXene, further reducing the AgNWs agglomeration probability.[64] These methods can significantly improve the stability and properties of AgNWs and MXene composites.

Using vacuum-assisted filtration and atomic layer deposition techniques, Xing et al. successfully prepared ultrathin MXene@AgNW@MoS_2 (MAM) composite films with excellent electromagnetic shielding performance, resembling a marbled structure.[65] When the thickness of the MAM film was 0.03 mm, the electromagnetic shielding effectiveness in the X-band reached 86.3 dB. This was attributed to forming a skeleton through the staggered arrangement of AgNWs dispersed within MXene flakes, constructing a doped layer with a three-dimensional network structure, effectively enhancing the film's conductivity. Vacuum-assisted filtration achieved alternating stacking of MXene/AgNW doped layers and AgNW single layers, forming a layered structure with multiple heterogeneous interfaces. These interfaces induce interface polarization, increasing multiple electromagnetic wave reflections and scattering, thereby enhancing electromagnetic wave loss. Wang et al. successfully prepared MXene/chitosan/silver nanowires (AgNW) sandwich films by vacuum-assisted filtration, in which the AgNW core layer was adjacent to two MXene/chitosan layers.[66] The results showed that the electromagnetic shielding value of the sandwich film was 82.3 dB. When the contents of AgNW and MXene were both 33.3%, the electromagnetic shielding efficiency of the sandwich film was 26.167 $dB{\cdot}cm^{-1}$ compared with its thickness, which was far higher than that of inorganic hybrid composites and polymer composites filled with hybrid fillers. EMI shielding often relies on advanced material designs to mitigate interference effectively. One such innovative approach involves utilizing sandwich structures, which offer enhanced shielding capabilities through strategic layering. Building upon this concept, Yang et al. successfully prepared an EMI shielding film with a sandwich structure using electrospinning and vacuum-assisted filtration technology, using a polyvinylidene fluoride layer and a conductive filler layer containing AgNW and MXene as raw materials.[67] The results showed that when the AgNW mass fraction was 1.28 wt %, the electromagnetic shielding effectiveness of the film reached 45.4 dB. Even after 2000 bending cycles, the electromagnetic shielding effectiveness only slightly decreased, demonstrating its excellent mechanical performance and stability. This was attributed to the independent AgNW layer endowing the film with primary electromagnetic shielding performance at low conductive filler contents. Qu et al. successfully prepared a multiheterolayer high-performance flexible electromagnetic shielding functional composite (AMA composite) using nanosilver sheets (as a reflector), MXene (as a loss layer), and silver nanowires (as a heat conduction and shielding layer).[68] The EMI SE of MXene coating with different temperatures and thicknesses is shown in Figure 6a–6b, respectively. The results showed that with a coating weight of only 25 $g{\cdot}m^{-2}$, the EMI shielding value of the composite material reached 70.96 dB, surpassing commercial standards. After soaking for 6 h, the average electromagnetic shielding efficiency decreased slightly. In EMI shielding, the development of advanced composite coatings has garnered significant attention. Researchers have been diligently exploring advanced coating strategies. Chang et al. prepared MXene/AgNWs/PEDOT composite coating using drip casting in this pursuit.[69] The electromagnetic shielding effectiveness of MXene/AgNWs/PEDOT composite coatings with different MXene contents was investigated. The coating with 76.6 wt % MXene/AgNWs/PEDOT: PSS showed the best performance, and it was subjected to a bending test, as shown in Figure 6c. The test results indicated that even after 800 bending cycles, the electromagnetic interference shielding performance of this coating exhibited high resistance to bending cycle stability. The electromagnetic shielding effectiveness of the coating at a thickness of 10 μm was 31.5 dB, far exceeding most reported coatings of similar thickness in polymer-based electromagnetic shielding composite materials. Cheng et al. coated the core material of transparent wood (TW) with AgNW @MXene.[70] The research showed that the composite material's average electromagnetic shielding effectiveness value reached 44.0 dB under the X-band. This performance improvement was attributed to multiple reflections of electromagnetic waves within the microchannels of the TW layer and increased absorption shielding caused by interface polarization between AgNW and MXene.

Due to their elevated conductivity, intelligent and structured hybrid materials significantly meet the demand for eliminating unnecessary EMI. A triadic composite nanostructure comprising MXene (Nb_2CT_x and $Ti_3C_2T_x$), metal oxide (Nb_2O_5), and silver (Ag) was fabricated by Rajavel et al.[73] The maximum total shielding effect of the Nb_2CT_x/Nb_2O_5–Ag hybrid assembly at 1 mm thickness was 68.76 dB in the X-band and 72.04 dB in the Ku-band, respectively. The substantial enhancement in electromagnetic shielding performance of the triadic nanostructure was attributed to its robust electrical conductivity and interface polarization among the triadic interfaces, along with multiple reflection losses. The synergistic interplay of metallic silver nanoparticles, semiconductor metal oxides, and conductive layered multilayers results in conduction losses, polarization effects, and multiple reflections of incident radiation, facilitating the complete dissipation of electromagnetic waves. Despite the high conductivity of MXene fibers, the poor spinnability of pure MXene dispersion and the brittleness of conductive fibers limit their application. Here, Liu et al. adopted the coaxial wet spinning assembly strategy to prepare MXene-based core–shell fibers with mechanical strength and electrical conductivity, using regenerated cellulose (RC) as the ductile component and graphene oxide/MXene (GM) as the conductive component.[71] The EMI shielding mechanism is illustrated in Figure 6d. By optimizing the structural design, hollow fibers of RC@GM90 exhibited a strength of 134.7 MPa, a high toughness of 14.1 $MJ{\cdot}m^{-3}$, a fracture elongation of 13%, and a high electrical conductivity of 2.37×103 $S{\cdot}m^{-1}$. When stitched onto textile substrates, hollow RC@ MXene fibers with a high electrical conductivity of 3.68×104 $S{\cdot}m^{-1}$ provided over 90 dB of extraordinary EMI shielding efficiency. Yang et al. investigated the influence of the proportion and loading amount of MoO_3/PDA and MXene nanosheets on microwave absorption performance.[74] When the ratio of the two is 3:1, Mo_2C/NC@MXene-2 showed the best absorption performance at 25% load.

https://doi.org/10.1021/acsami.4c11189
ACS Appl. Mater. Interfaces XXXX, XXX, XXX–XXX

Duan et al. prepared MXene/carbon fiber fabric/thermoplastic polyurethane (MXene/CFf/TPU) composites by atomizing deposition, layer-by-layer stacking, and hot pressing techniques.[75] The electromagnetic shielding performance of the MXene/CFf/TPU composite increased with the MXene mass fraction up to 40.4 dB, which can be attributed to the dielectric loss provided by the conductive filler and the enhanced absorption effect within the sandwich structure. Even after multiple bending and releasing cycles, the composite material maintained excellent tensile properties, electromagnetic shielding stability, and flexibility. Li et al. employed a high-efficiency vacuum filtration-assisted spray coating technique to successfully fabricate polyaniline (PANI)/MXene/cotton fabric (PMCF).[76] PMCF exhibited high sensitivity to ammonia, reaching 19.6% at a concentration of 200 ppm. By optimizing the decorative structure of PANI/MXene coating on cotton fabric, the electromagnetic shielding efficiency value was as high as 54 dB. More importantly, PMCF can adaptively act as the "switch" of electromagnetic shielding and achieve effective, strong shielding from 24 dB to inefficient, weak shielding from 15 dB under hydrogen chloride and ammonia vapor stimulation. Ma et al. prepared SiC nanowires (SiCnw) /MXene heterogeneous nanostructures in polyvinylidene fluoride matrix by electrostatic self-assembly.[77] The presence of numerous stacking defects of MXene nanosheets and SiCnw in the structure effectively generates many heterogeneous interfaces in the polymer matrix, thereby significantly enhancing electromagnetic wave absorption performance. By optimizing the ratio of SiCnw to MXene (7:1) and the concentration of SiCnw/MXene (20 wt %), an adequate bandwidth of 5.0 GHz in the Ku-band was achieved. The flexible PVDF/SiCnw/MXene nanocomposites had excellent electromagnetic wave absorption properties due to appropriate impedance matching, enhanced interfacial polarization, and high dielectric loss. Conductive polymer composite materials (CPCs) have garnered significant attention in EMI shielding. However, these materials face an inherent contradiction between high electromagnetic wave absorption and low electromagnetic wave reflection. Ma et al. employed a layer-by-layer vacuum filtration method to construct excellent electromagnetic wave absorption and low electromagnetic wave reflection composite films with controllable magnetic induction double-gradient structures using cellulose nanofibers (CNF), MXene, and FeCo, as illustrated in the shielding mechanism diagram (Figure 6e).[72] The electromagnetic shielding effectiveness of the composite film reached 58.0 dB, with a reflection coefficient as low as 0.61. Due to the synergistic effect of the transition layer and the gradient-structured reflection layer, the composite film exhibits favorable impedance matching, abundant loss mechanisms, and efficient electromagnetic shielding capability, resulting in absorption-dominated shielding characteristics. Additionally, the gradient structure facilitates an "absorption−reflection-reabsorption" process when electromagnetic waves propagate to the composite film.

The simple enhancement of electrical conductivity in electromagnetic shielding materials may lead to intense reflection of electromagnetic waves, triggering secondary electromagnetic pollution while overlooking the electromagnetic wave losses caused by internal scattering. MXene materials can be prepared into porous electromagnetic shielding materials without affecting themselves.[78] They exhibit efficient electromagnetic wave absorption capabilities, lightweight characteristics, flexibility, and pliability without compromising their inherent properties. Formats such as foams, aerogels, and hydrogels are mentioned, highlighting their controllable pore size and porosity, excellent thermal resistance, and chemical stability. The porous structure of MXene materials provides ample surface area and pore space, enabling outstanding performance in electromagnetic shielding. Moreover, they possess portability, durability, and customizability advantages, making them suitable for various application scenarios and aligning with sustainability requirements.

Polymeric materials, due to their inherent low electrical conductivity and relatively poor electromagnetic shielding performance, often struggle to meet the high shielding effectiveness required for applications when used alone.[79] Moreover, to achieve effective electromagnetic shielding, polymer-based materials typically require elaborate structural designs, such as segregated structures, layered structures, and foam structures, as well as constructing a three-dimensional conductive network to enhance their shielding capabilities.[80] These processes are not only technically demanding but may also necessitate a high volume of conductive fillers, which could adversely affect the mechanical properties and processability of the material.[81] Therefore, to overcome these limitations and enhance the electromagnetic shielding performance of polymers, researchers often combine polymers with substances like MXene, which have high conductivity and excellent electromagnetic properties.[82] Through this composite strategy, not only can the electromagnetic characteristics of MXene be utilized to enhance both reflective and absorptive losses, but also the optimization of structure and morphology can lead to more efficient electromagnetic shielding effects, thereby developing new types of electromagnetic shielding materials that are both lightweight and highly effective. Li et al. prepared polyvinylidene fluoride/cobalt (Co)/MXene composite foam.[83] The introduced MXene portion was oxidized and converted into TiO_2 and amorphous carbon. The formed TiO_2 provided additional heterogeneous interfaces and capacitor-like structures conducive to dielectric polarization and reduced the excessive electrical conductivity of the original MXene, aiding impedance matching. Consequently, with a filler content of only 12 wt % (6 wt % MXene and 6 wt % Co), the electromagnetic wave absorption performance of the composite foam was enhanced. Research findings indicated that the composite foam exhibits applicable impedance matching, enhanced electromagnetic wave absorption, and high-performance thermal conduction properties. As representative materials are primarily driven by absorption for EMI shielding, they are more favored than traditional materials, primarily driven by reflection, especially in managing the increasingly severe electromagnetic radiation pollution. This preference stems from that materials primarily driven by absorption effectively reduce secondary pollution caused by reflected electromagnetic waves and balance high-efficiency electromagnetic shielding performance, presenting distinct advantages. Wang et al. fabricated porous three-dimensional MCF/epoxy EMI shielding nanocomposites through sol−gel followed by thermal reduction and vacuum-assisted impregnation solidification processes.[84] When the mass fraction of MCF was 4.25 wt % (MCF-5), the optimal electrical conductivity and maximum electromagnetic shielding value of MCF-5/epoxy nanocomposites were 184 $S \cdot m^{-1}$ and 46 dB, respectively, which were 3.1 × 104 and 4.8 times higher than

https://doi.org/10.1021/acsami.4c11189
ACS Appl. Mater. Interfaces XXXX, XXX, XXX−XXX

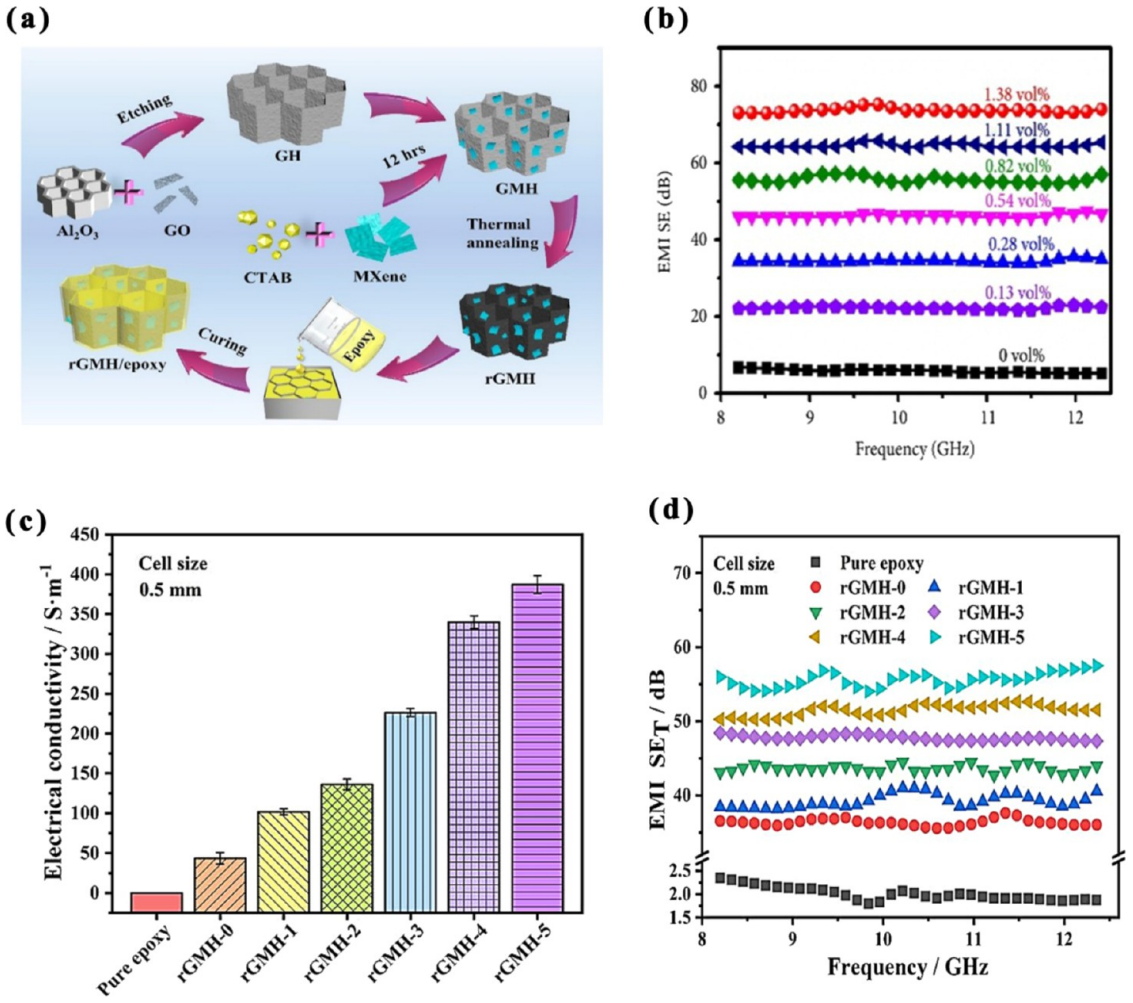

Figure 7. (a) Schematic diagram for fabricating rGMH/epoxy nanocomposites. Reproduced with permission from ref 95. Copyright 2020 Elsevier. (b) EMI SE values of the TCTA/epoxy nanocomposites at X-band. Reproduced with permission from ref 87. Copyright 2020 Research. (c) σ value of the rGMH/epoxy nanocomposites with 0.5 mm cell sizes. (d) EMI SE_T value of the rGMH/epoxy nanocomposites with 0.5 mm cell sizes. Reproduced with permission from ref 95. Copyright 2020 Elsevier.

those of MCF-0/epoxy nanocomposites (without MXene). The conductive network achieved electromagnetic wave attenuation and dissipation through multiple reflections and reabsorption, with absorption being the primary shielding mechanism. Cheng et al. successfully prepared MXene/AgNW/PU composite foam films by combining AgNWs and MXene into a PU matrix.[85] At a low density of 0.15 g·cm^{-3}, the three-dimensional conductive network of AgNWs and MXene, along with the porous structure and multiple interfaces, collectively facilitated achieving a high shielding efficiency of 50 dB in the X-band, with an 86% dominance of high absorption-driven shielding efficiency. At Ku-band frequencies, the composite foam film exhibited a higher shielding efficiency of 60 dB, with an absorption efficiency as high as 95%, demonstrating outstanding absorption-driven shielding performance. Even after 1000 cycles of compression and release, the composite foam film maintained an excellent electromagnetic shielding efficiency of 41.5 dB.

Huang et al. utilized trace hydroxyethyl cellulose as a gel to construct MXene aerogel through freeze-drying techniques, incorporating organic silicone resin into the MXene aerogel to form a stable and highly conductive network.[86] The doping of organic silicone in the MXene EMI shielding composite material achieved a conductivity of 3166.4 S·m^{-1}. In the X-band, the electromagnetic shielding effectiveness reached 74.5 dB. Wang et al. prepared a three-dimensional highly conductive cellulose nanofiber (CNF)/MXene aerogel (CTA) with a directional porous structure using freeze-drying techniques.[87] Subsequently, thermally treated CTA/epoxy nanocomposites (TCTA) were prepared through heat treatment, vacuum-assisted impregnation, and curing. EMI SE value of the TCTA/epoxy nanocomposites at X-band, as shown in Figure 7b. The results indicated that at an MXene volume fraction of 1.38 vol %, the electrical conductivity of TCTA/epoxy nanocomposites reached 74 dB. Yan et al. developed a "sandwich" structured MXene/aramid nanofiber (ANF)/carbon nanotube (CNT) aerogel.[88] Due to the one-dimensional nanostructure of carbon nanotubes and the two-dimensional layered structure of MXene,[89] these structures can increase the scattering and multiple reflections of electromagnetic waves within the material,[90] extending the propagation path of the electromagnetic waves and improving the absorption efficiency.[91,92] Therefore, carbon nanotubes and MXene contribute to the absorption and reflection of electromagnetic waves.[93] Although the thickness and density of the composite aerogel are only 2 mm and 0.0428 g·cm^{-3},

https://doi.org/10.1021/acsami.4c11189
ACS Appl. Mater. Interfaces XXXX, XXX, XXX−XXX

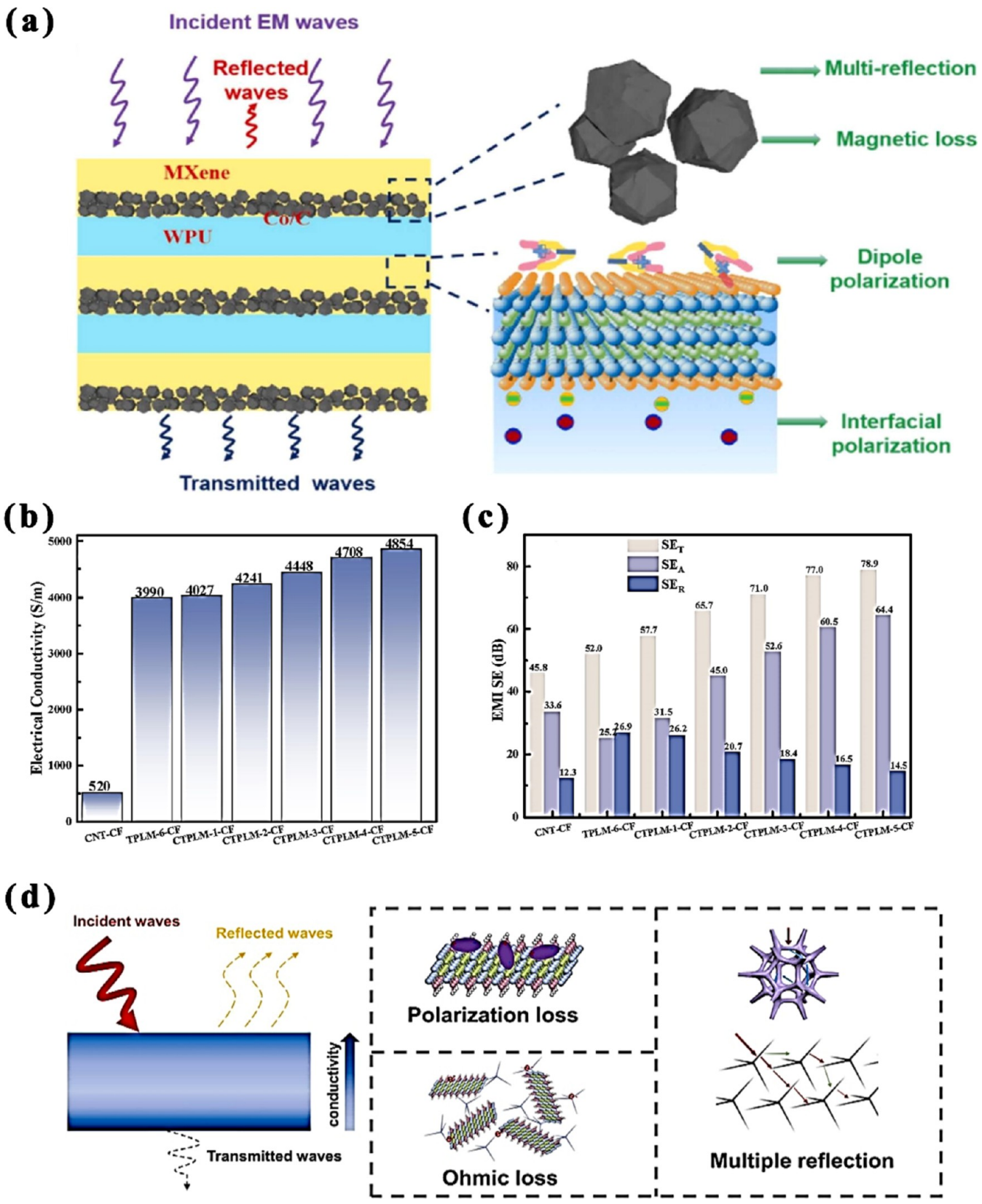

Figure 8. (a) EMI shielding mechanism of MXene-WPU-Co/C. EMI is shielding performance of CNT-CF, TPLM-CF, and CTPLM-CF. Reproduced with permission from ref 100. Copyright 2023 Elsevier. (b) Conductivity and (c) average values of EMI SE. Reproduced with permission from ref 103. Copyright 2022 Elsevier. (d) Potential schematic of the shielding mechanism of M_2A_nF composite foam. Reproduced with permission from ref 104. Copyright 2023 Elsevier.

respectively, the electromagnetic shielding effectiveness in the X-band reached 69.0 dB. Zou et al. prepared an iron oxide/carbon nanotube/waterborne polyurethane (Fe_3O_4/CNTs/WPU) aerogel and then coated the bottom with MXene to

https://doi.org/10.1021/acsami.4c11189
ACS Appl. Mater. Interfaces XXXX, XXX, XXX−XXX

create an asymmetric structure.[94] Additionally, during the MXene-Fe_3O_4 coating process, a medium or transition layer was formed through gravity and the capillary action of the aerogel. This clever design presented distinct absorption, transition, and reflection layers following the principles of progressive modular design. The composite aerogel exhibited an average electromagnetic shielding effectiveness of 20.06 dB in the X-band, with a low reflectance of 0.396. With an MXene content of only 2.35 vol %, the SSE/t was 332.60 $dB{\cdot}cm^2{\cdot}g^{-1}$. Song et al. self-assembled MXene on reduced graphene oxide (rGO) through electrostatic adsorption, added epoxy resin, and formed a honeycomb-structured rGO-MXene/epoxy resin nanocomposite, as depicted in Figure 7a.[95] The synergistic effect of rGO and MXene significantly enhanced the composite material's electrical conductivity and electromagnetic shielding effectiveness. Under the same MXene filling amount, the composite material's electrical conductivity and electromagnetic shielding effectiveness shows a decreasing trend as the honeycomb pore size increases. First, a smaller honeycomb pore size helps the MXene layers to form more continuous and close contact, building an efficient conductive network and thereby improving the overall electrical conductivity of the material.[18] Second, the small pore size in the honeycomb structure is beneficial for increasing the scattering and absorption opportunities of electromagnetic waves in the material, extending their propagation path and thus enhancing the absorption efficiency.[96] When using a 0.5 mm unit size, the conductivity was 387.1 $S{\cdot}m^{-1}$, and the electromagnetic shielding effectiveness was 55 dB, showing a significant improvement, as illustrated in Figure 7c−7d, respectively. Wang et al. prepared a three-dimensional $Ti_3C_2T_x$ Mxene/Sodium Alginate (SA)/Multi-Walled Carbon Nanotubes (MWCNTs) phase change material using a controllable directional freezing method.[97] This method constructs an orderly porous structure that allows incident electromagnetic waves to reflect and scatter multiple times within the phase-change material. Introducing multiwalled carbon nanotubes into the MSC phase change material can form a three-dimensional conductive network with Mxene, enhancing its conductivity and electromagnetic shielding performance.

5. MXENE-BASED FOUR-ELEMENT COMPOSITE ELECTROMAGNETIC SHIELDING MATERIAL

Excessive electromagnetic radiation generated during the operation of electronic devices disrupts the normal functioning of precision electronic instruments and poses potential risks to human health.[98] Most existing electromagnetic shielding materials work through the reflection mechanism, leading to secondary severe electromagnetic wave pollution. Multiple components are advantageous for introducing various loss mechanisms.[99] Researchers usually composite various loss components to prepare high-performance electromagnetic shielding materials and introduce mechanisms other than electrical loss, dielectric loss, and magnetic loss (such as multiple reflections, interface polarization, dipole polarization, etc.). With deep research and continuous technological improvements, MXene-based quaternary composite electromagnetic shielding materials have emerged as a prominent research focus.

Zhang et al. synthesized a multilayered composite film, MXene-WPU-Co/C, with controllable thickness and reflectivity using Co/C magnetic particles, environmentally friendly waterborne polyurethane (WPU), and MXene as raw materials.[100] The shielding mechanism is illustrated in Figure 8a. The results showed that when the thickness of the composite film was 0.2 mm. The mass fraction of MXene was only 10 wt %, the X-band electromagnetic shielding efficiency was 31 dB, and the reflectance was 0.01, indicating that the SE_T of the composite film mainly depends on the SE_A rather than the SE_R. Compared to similar electromagnetic shielding materials, this novel, low-cost, controllable design strategy provided a new approach for developing high-performance, efficient, and low-reflectivity electromagnetic shielding films. Guo et al. employed a simple two-step vacuum filtration method to fabricate a film composed of low-conductivity $CoFe_2O_4$@MXene/CNF layers and high-conductivity silver nanowires (AgNWs)/CNF layers.[101] When the thickness of the composite film was only 0.1 mm, the electromagnetic shielding efficiency was as high as 73.3 dB, the average electromagnetic shielding efficiency was 70.9 dB, and the reflection efficiency was only 4.9 dB. This was attributed to the rational arrangement of impedance-matching and shielding layers and the synergistic effects of electrical and magnetic losses. Li et al. prepared PFDT/CB/MXene@ Paper composites using a simple coating technique.[102] The results showed that the electromagnetic shielding performance of the paper-based functional materials could be maintained well under multiple cyclic bending conditions and in different acid, alkali, and ultraviolet environments, which significantly improved the applicability of the paper-based functional materials. This study provided an efficient design strategy for preparing high-performance paper-based electromagnetic shielding materials.

Ma et al. successfully designed well-structured asymmetric gradient multilayer composite films by establishing controllable electromagnetic gradients.[105] Cellulose nanofibers were used as the matrix, and a layer-by-layer filtration method was employed to distribute FeCo@ rGO and MXene fillers evenly, forming an ordered multilayer structure with alternating conductive and magnetic gradients. Due to the gradient absorption, shielding, and reflection mechanisms of electromagnetic waves within the film layers, the electromagnetic shielding effectiveness of the symmetric gradient alternating 6-layer composite film reached 45.2 dB in the X-band, with a reflection coefficient decreasing to 0.71 when 20 wt % filler was added. This strategy provided a feasible approach to designing tunable electromagnetic shielding composite materials, holding significant practical implications for expanding the applications of MXene-based composite materials. Zhu et al. successfully synthesized Fe_3O_4-modified carbon nanotube (Fe_3O_4@CNT)/MXene/cross-linked aramid nanofiber (c-ANF)/polyimide (PI) aerogels with a three-dimensional ordered hierarchical porous structure using a unidirectional freezing method.[106] The composite aerogel's electromagnetic shielding effectiveness and microwave reflection, with 8 wt % each of Fe_3O_4@CNTs and MXene, was remarkably high at 67.42 and 0.60 dB, respectively. Li et al. utilized a simple solution impregnation technique to create a conductive fabric modified with CNT/MXene/polyaniline/$LiMn_2O_4$ (CTPLM).[103] The electromagnetic shielding effectiveness of the fabric reached 78.9 dB with a thickness of 0.27 mm, and the absorption shielding efficiency within the 8.2−12.4 GHz range was as high as 64.4 dB (Figure 8b−8c). The synergistic effect of high conductivity and a porous structure made the CTPLM-CF textile exhibit significantly higher electromagnetic shielding performance than the original MXene membrane and pure CNT layer.

https://doi.org/10.1021/acsami.4c11189
ACS Appl. Mater. Interfaces XXXX, XXX, XXX−XXX

Furthermore, combining 3 layers of conductive fabric further enhanced the electromagnetic shielding performance to 104.3 dB. Electromagnetic wave absorption (EMWA) materials, with their low cost and high efficiency, are of great value in addressing the challenges of electromagnetic wave pollution. Hou et al. CoNi@C@$Ti_3C_2T_x$/TiO_2 nanocomposites (CNCTT) were successfully synthesized by solvothermal method, electrostatic self-assembly, and heat treatment using CoNi-MOF@$Ti_3C_2T_x$ as raw material.[107] By adjusting the proportion of magnetic metal sources, the regulation effect of CNCTT nanocomposites on electromagnetic wave absorption was studied. The multilevel porous structure promoted interface polarization through the quadruple CNCTT interface, enhanced magnetic loss through the coupling network of CoNi nanoparticles, increased conduction loss through the graphite carbon layer/$Ti_3C_2T_x$/TiO_2 triple network, and optimized impedance matching through the synergistic effect of dielectric and magnetic losses. Li et al. successfully synthesized a multilayer composite CoFe-K/GC@MnO_2@MXene (CMM) using electrostatic self-assembly technology.[108] CMM exhibited outstanding electromagnetic wave absorption performance, attributed to higher conduction loss levels, enhanced interface polarization, and optimized impedance matching. Zou et al. prepared MXene/Ag@ZnO/WPU/melamine formaldehyde (MF) composite foam via simple unidirectional evaporation combined with a vacuum drying method.[104] The shielding mechanism, as depicted in Figure 8d: the top has a good impedance matching, allowing electromagnetic waves to enter the material, and the bottom is an effective conductive network, ensuring that the composite foam has a high electromagnetic shielding performance. Under the "absorption−reflection-reabsorption" mechanism, when the volume fractions of MXene and Ag were 2.72 and 4.25%, respectively, the electromagnetic shielding effectiveness of the composite material reached 39.90 dB, with a reflection coefficient of 0.1423, providing a new solution for the large-scale preparation of high-performance electromagnetic shielding materials with absorption-dominant characteristics. Wang et al. prepared BC/MXene/MSiCnw/FRTPU aerogel composites by vacuum-assisted impregnation.[109] When the mass fraction of MXene was 6.17 wt %, the electromagnetic shielding utilization efficiency of the aerogel composite material reached 1209.08 $dB{\cdot}gg^{-1}$, and the average electromagnetic shielding effectiveness in the K-band was as high as 81.6 dB. Moreover, due to the synergistic effect among MXene, MSiCnw, and FRTPU, the aerogel composite material exhibited excellent fire resistance (reducing PHRR by 69.8%), surpassing most other aerogel materials. The multifunctional aerogel composite material showed promising electromagnetic shielding and thermal insulation prospects.

6. CONCLUSIONS

The paper provides a systematic summary and analysis of the multilevel research on MXene-based composite electromagnetic shielding materials, covering unary, binary, ternary, and quaternary composite systems. First, we extensively discuss the current research status of MXene as a unary electromagnetic shielding material, emphasizing its outstanding conductivity and electromagnetic shielding performance. Furthermore, we focus on binary composite structures constructed with MXene and polymers, carbon derivatives, and ferrites, among others, analyzing the effects of various combinations on electromagnetic shielding performance. In addition, the research status of MXene-based ternary composite electromagnetic shielding materials is introduced. Lastly, the paper explores the research progress of MXene-based quaternary composite electromagnetic shielding materials, demonstrating the synergistic effects of multicomponent structures.

However, despite the excellent performance of MXene-based composite electromagnetic shielding materials, there are still some shortcomings and challenges. One of the main challenges is that although considerable experimental research has been conducted, the theoretical understanding of the interaction mechanisms and composite effects between MXene and other components still needs to be improved. This has led to certain limitations in material design and performance optimization. Another challenge is that existing research primarily focuses on the electromagnetic shielding performance within specific frequency ranges, with relatively fewer studies on wideband shielding performance. This limits the applicability of such materials in practical scenarios. Additionally, although some fabrication methods exist, the scalability and reproducibility of MXene-based composite materials still need to be improved. The demands for large-scale production and engineering applications have yet to be effectively addressed. Furthermore, insufficient research on the stability and durability of materials under different environmental conditions may constrain their reliability and longevity in practical applications. Lastly, current research primarily concentrates on the electromagnetic shielding performance of MXene-based composite materials, with fewer studies on multifunctional material design. Therefore, to overcome these shortcomings, there is a need for further theoretical exploration, experimental validation, and engineering applications, along with interdisciplinary collaboration and communication, to propel the development of MXene-based composite electromagnetic shielding materials.

Future research can first focus on the multifunctional design of MXene-based composite electromagnetic shielding materials. For example, it integrates the electromagnetic shielding performance of MXene with other properties such as mechanical strength, thermal conductivity, and optical properties to achieve material multifunctionality. Furthermore, there should be an emphasis on expanding the electromagnetic shielding performance of MXene-based composite materials across different frequency ranges to make them suitable for a broader range of application scenarios, including high-frequency and low-frequency electromagnetic waves. Additionally, there should focus on the sustainability and environmental friendliness of MXene-based composite electromagnetic shielding materials. This involves seeking biodegradable matrix materials, environmentally friendly synthesis methods, and recyclable components to meet green requirements. Finally, the research focus should gradually shift from the laboratory to practical application scenarios, including electronic devices, communication systems, and military applications. Material reproducibility, stability, and cost must be thoroughly considered in real-world engineering applications. This will enable MXene-based composite electromagnetic shielding materials to meet better the practical requirements in future electromagnetic shielding applications in communication, electronic devices, and defense, laying the foundation for designing and applying the next generation of high-performance electromagnetic shielding materials.

https://doi.org/10.1021/acsami.4c11189
ACS Appl. Mater. Interfaces XXXX, XXX, XXX−XXX

AUTHOR INFORMATION

Corresponding Author

Yuanjun Liu − *School of Textile Science and Engineering, Tianjin Key Laboratory of Advanced Textile Composites, and Tianjin Key Laboratory of Advanced Fiber and Energy Storage Technology, Tiangong University, Tianjin 300387, China*; Email: liuyuanjunsd@163.com

Authors

Yi Liu − *School of Textile Science and Engineering, Tiangong University, Tianjin 300387, China*; orcid.org/0009-0005-3058-9308

Xiaoming Zhao − *School of Textile Science and Engineering, Tianjin Key Laboratory of Advanced Textile Composites, and Tianjin Key Laboratory of Advanced Fiber and Energy Storage Technology, Tiangong University, Tianjin 300387, China*

Complete contact information is available at: https://pubs.acs.org/10.1021/acsami.4c11189

Author Contributions

Yi Liu: Conceptualization, Data curation, Formal analysis, Methodology, Writing original draft, Investigation. Yuanjun Liu: Methodology, Supervision, Validation, Funding acquisition, Writing-review and editing. Xiaoming Zhao: Resources, Visualization, Funding acquisition.

Notes

The authors declare no competing financial interest.

ACKNOWLEDGMENTS

This work was supported by the Consulting Research Project of the Chinese Academy of Engineering [2021DFZD1].

REFERENCES

(1) Morrison, J. Electronics' noise disorients migratory birds. *Nature* **2014**, *146*, 15176−15178.

(2) Lavine, M. S. Flexible and lightweight shielding. *Science* **2016**, *353*, 1109−1110.

(3) Han, M.; Gogotsi, Y. Perspectives for electromagnetic radiation protection with MXenes. *Carbon* **2023**, *204*, 17−25.

(4) Iqbal, A.; Shahzad, F.; Hantanasirisakul, K.; Kim, M. K.; Kwon, J.; Hong, J.; Kim, H.; Kim, D.; Gogotsi, Y.; Koo, C. M. Anomalous absorption of electromagnetic waves by 2D transition metal carbonitride Ti_3CNT_x (MXene). *Science* **2020**, *369*, 446−450.

(5) Guan, H.; Chung, D. D. L. Radio-wave electrical conductivity and absorption-dominant interaction with radio wave of exfoliated-graphite-based flexible graphite, with relevance to electromagnetic shielding and antennas. *Carbon* **2020**, *157*, 549−562.

(6) Liu, J.; Yu, M. Y.; Yu, Z. Z.; Nicolosi, V. Design and advanced manufacturing of electromagnetic interference shielding materials. *Mater. Today* **2023**, *66*, 245−272.

(7) Liu, Y.; Wang, Y.; Wu, N.; Han, M.; Liu, W.; Liu, J.; Zeng, Z. Diverse structural design strategies of MXene-based macrostructure for high-performance electromagnetic interference shielding. *Nano-Micro Lett.* **2023**, *15*, No. 240.

(8) Albert, A. A.; Parthasarathy, V.; Kumar, P. S. Review on recent progress in epoxy-based composite materials for electromagnetic interference (EMI) shielding applications. *Polym. Compos.* **2024**, *45*, 1956−1984.

(9) Zong, J. Y.; Cao, M. S. Graphene-like MXene-based microwave absorbers and shields: latest progress and perspectives. *Mater. Today Phys.* **2024**, *43*, No. 101400.

(10) Song, Q.; Ye, F.; Kong, L.; Shen, Q.; Han, L.; Feng, L.; Li, H.; et al. Graphene and MXene nanomaterials: toward high-performance electromagnetic wave absorption in gigahertz band range. *Adv. Funct. Mater.* **2020**, *30*, No. 2000475.

(11) Naguib, M.; Kurtoglu, M.; Presser, V.; Lu, J.; Niu, J.; Min, H.; Hultman, L.; Gogotsi, Y.; Barsoum, M. W. Two-dimensional nanocrystals produced by exfoliation of Ti_3AlC_2. *Adv. Mater.* **2011**, *23*, 4248−4253.

(12) VahidMohammadi, A.; Rosen, J.; Gogotsi, Y. The world of two-dimensional carbides and nitrides (MXenes). *Science* **2021**, *372*, No. eabf1581.

(13) Anasori, B.; Lukatskaya, M. R.; Gogotsi, Y. 2D metal carbides and nitrides (MXenes) for energy storage. *Nat. Rev. Mater.* **2017**, *2*, No. 1226419.

(14) Ahmad, N.; Rasheed, S.; Mohyuddin, A.; Fatima, B.; Nabeel, M. I.; Riaz, M. T.; Ul Haq, M. N.; Hussain, D. 2D MXenes and their composites; design, synthesis, and environmental sensing applications. *Chemosphere* **2024**, *352*, No. 141280.

(15) Wang, L.; Cheng, J.; Zou, Y.; Zheng, W.; Wang, Y.; Liu, Y.; Zhang, H.; Zhang, D.; Ji, X. Current advances and future perspectives of MXene-based electromagnetic interference shielding materials. *Adv. Compos. Hybrid Mater.* **2023**, *6*, No. 172.

(16) Kumar, R.; Sahoo, S.; Joanni, E.; Shim, J. J. Cutting edge composite materials based on MXenes: synthesis and electromagnetic interference shielding applications. *Composites, Part B* **2023**, *264*, No. 110874.

(17) Oliveira, F. M.; Azadmanjiri, J.; Wang, X.; Yu, M.; Sofer, Z. Structure design and processing strategies of MXene-based materials for electromagnetic interference shielding. *Small Methods* **2023**, *7*, No. 2300112.

(18) Verma, R.; Thakur, P.; Chauhan, A.; Jasrotia, R.; Thakur, A. A review on MXene and its' composites for electromagnetic interference (EMI) shielding applications. *Carbon* **2023**, *208*, 170−190.

(19) Liu, H.; Wang, Z.; Wang, J.; Yang, Y.; Wu, S.; You, C.; Tian, N.; Li, Y. Structural evolution of MXenes and their composites for electromagnetic interference shielding applications. *Nanoscale* **2022**, *14*, 9218.

(20) Tang, X.; Zhou, M. MXene-based electromagnetic wave response. *J. Phys.: Energy* **2021**, *3*, No. 042001.

(21) Shahzad, F.; Alhabeb, M.; Hatter, C. B.; Anasori, B.; Hong, S. M.; Koo, C. M.; Gogotsi, Y. Electromagnetic interference shielding with 2D transition metal carbides (MXenes). *Science* **2016**, *353*, 1137−1140.

(22) Raagulan, K.; Braveenth, R.; Jang, H. J.; Lee, Y. S.; Yang, C. M.; Kim, B. M.; Moon, J. J.; Chai, K. Y. Electromagnetic shielding by MXene-graphene-PVDF composite with hydrophobic, lightweight and flexible graphene coated fabric. *Materials* **2018**, *11*, 1803.

(23) Liu, J.; Zhang, H. B.; Sun, R.; Liu, Y.; Liu, Z.; Zhou, A.; Yu, Z. Z. Hydrophobic, flexible, and lightweight MXene foams for high-performance electromagnetic-interference shielding. *Adv. Mater.* **2017**, *29*, No. 1702367.

(24) Yun, T.; Kim, H.; Iqbal, A.; Cho, Y. S.; Lee, G. S.; Kim, M. K.; Kim, S. J.; Kim, D.; Gogotsi, Y.; Kim, S. O.; Koo, C. M. Electromagnetic interference shielding: electromagnetic shielding of monolayer MXene assemblies. *Adv. Mater.* **2020**, *32*, No. 2070064.

(25) Wan, Y. J.; Rajavel, K. X.; Li, M.; Wang, X. Y.; Liao, S. Y.; Lin, Z. Q.; Zhu, P. L.; Sun, R.; Wong, C. P. Electromagnetic interference shielding of $Ti_3C_2T_x$ MXene modified by ionic liquid for high chemical stability and excellent mechanical strength. *Chem. Eng. J.* **2021**, *408*, No. 127303.

(26) Wan, S.; Li, X.; Chen, Y.; Liu, N.; Du, Y.; Dou, S.; Jiang, L.; Cheng, Q. High-strength scalable MXene films through bridging-induced densification. *Science* **2021**, *374*, 96.

(27) Zhang, X.; Wang, X.; Lei, Z.; Wang, L.; Tian, M.; Zhu, S.; Xiao, H.; Tang, X.; Qu, L. Flexible MXene-decorated fabric with interwoven conductive networks for integrated joule heating, electromagnetic interference shielding, and strain sensing performances. *ACS Appl. Mater. Interfaces.* **2020**, *12*, 14459.

(28) Xu, W.; Li, S.; Zhang, W.; Ouyang, B.; Yu, W.; Zhou, Y. Nitrogen-doped $Ti_3C_2T_x$ MXene induced by plasma treatment with

enhanced microwave absorption properties. *ACS Appl. Mater. Interfaces* **2021**, *13*, 49242.
(29) Ying, M.; Zhao, R.; Hu, X.; Zhang, Z.; Liu, W.; Yu, J.; Liu, X.; Liu, X.; Rong, H.; Wu, C.; Li, Y.; Zhang, X. Wrinkled titanium carbide (MXene) with surface charge polarizations through chemical etching for superior electromagnetic interference shielding. *Angew. Chem., Int. Ed.* **2022**, *61*, No. e202201323.
(30) Zhu, L. L.; Wu, W. W.; Chen, J. J.; Hu, Z. M.; Yu, J. R.; Wang, Y. High-performance electromagnetic wave absorption by two-dimensional mesoporous monolayer $Ti_3C_2T_x$ MXene. *Chem. Eng. J.* **2024**, *488*, No. 150649.
(31) Xia, B.; Wang, Z.; Wang, T.; Chen, S.; Wu, H.; Zhang, B.; Si, Y.; Chen, Z.; Li, B. W.; Kou, Z.; He, D. Bridging sheet size controls densification of MXene films for robust electromagnetic interference shielding. *iScience* **2022**, *25*, No. 105001.
(32) Yin, P. F.; Lan, D.; Lu, C. F.; Jia, Z. R.; Feng, A. L.; Liu, P. B.; Wang, J.; et al. Research progress of structural regulation and composition optimization to strengthen absorbing mechanism in emerging composites for efficient electromagnetic protection. *J. Mater. Sci. Technol.* **2025**, *204*, 204−223.
(33) Anand, S.; Vu, M. C.; Mani, D.; Kim, J. B.; Jeong, T.; Choi, W. K.; Won, J. C.; Kim, S. R. A continuous interfacial bridging approach to fabricate ultrastrong hydroxylated carbon nanotubes intercalated MXene films with superior electromagnetic interference shielding and thermal dissipating properties. *Adv. Compos. Hybrid Mater.* **2024**, *7*, No. 33.
(34) He, Z. J.; Zhang, W. R.; Zhang, J.; Xie, J. L.; Su, F. F.; Li, Y. C.; Zheng, Y. P.; et al. Enhancing the electromagnetic interference shielding of epoxy resin composites with hierarchically structured MXene/graphene aerogel. *Composites, Part B* **2024**, *274*, No. 111230.
(35) Han, M.; Shuck, C. E.; Singh, A.; Yang, Y.; Foucher, A. C.; Goad, A.; McBride, B.; May, S. J.; Shenoy, V. B.; Stach, E. A.; Gogotsi, Y. Efficient microwave absorption with $V_{n+1}C_nT_x$ MXenes. *Cell Rep. Phys. Sci.* **2022**, *3*, No. 101073.
(36) Kim, E.; Zhang, H.; Lee, J. H.; Chen, H.; Zhang, H.; Muhammad, H. J.; Shen, X.; Kim, J. K. MXene/polyurethane auxetic composite foam for electromagnetic interference shielding and impact attenuation. *Composites, Part A* **2021**, *147*, No. 106430.
(37) Idumah, C. I. Recent advancements in electromagnetic interference shielding of polymer and mxene nanocomposite. *Polymer* **2023**, *62*, 19.
(38) Zhai, J.; Cui, C.; Li, A.; Guo, R.; Cheng, C.; Ren, E.; Xiao, H.; Zhou, M.; Zhang, J. Waste cotton fabric/MXene composite aerogel with heat generation and insulation for efficient electromagnetic interference shielding. *Ceram. Int.* **2022**, *48*, 13464.
(39) Zhu, M.; Yan, X.; Xu, H.; Xu, Y.; Kong, L. Highly conductive and flexible bilayered MXene/cellulose paper sheet for efficient electromagnetic interference shielding applications. *Ceram. Int.* **2021**, *47*, 17234.
(40) Wei, Y.; Hu, C.; Dai, Z.; Zhang, Y.; Zhang, W.; Lin, X. Highly anisotropic MXene@wood composites for tunable electromagnetic interference shielding. *Composites, Part A* **2023**, *168*, No. 107476.
(41) Luo, J. Q.; Zhao, S.; Zhang, H. B.; Deng, Z.; Li, L.; Yu, Z. Z. Flexible, stretchable and electrically conductive MXene/natural rubber nanocomposite films for efficient electromagnetic interference shielding. *Compos. Sci. Technol.* **2019**, *182*, No. 107754.
(42) Zhou, Z.; Liu, J.; Zhang, X.; Tian, D.; Zhan, Z.; Lu, C. Ultrathin MXene/calcium alginate aerogel film for high-performance electromagnetic interference shielding. *Adv. Mater. Interfaces* **2019**, *6*, No. 1802040.
(43) Wu, N.; Li, B.; Pan, F.; Zhang, R.; Liu, J.; Zeng, Z. Ultrafine cellulose nanocrystal-reinforced MXene biomimetic composites for multifunctional electromagnetic interference shielding. *Sci. China Mater.* **2023**, *66*, 1597.
(44) Feng, S.; Zhan, Z.; Yi, Y.; Zhou, Z.; Lu, C. Facile fabrication of MXene/cellulose fiber composite film with homogeneous and aligned structure via wet co-milling for enhancing electromagnetic interference shielding performance. *Composites, Part A* **2022**, *157*, No. 106907.
(45) Hu, Y.; Chen, J.; Yang, G.; Li, Y.; Dong, M.; Zhang, H.; Bilotti, E.; Jiang, J.; Papageorgiou, D. G. Highly conductive and mechanically robust MXene@CF core-shell composites for in-situ damage sensing and electromagnetic interference shielding. *Compos. Sci. Technol.* **2024**, *246*, No. 110356.
(46) Xu, Z.; Ding, X.; Li, S.; Huang, F.; Wang, B.; Wang, S.; Zhang, X.; Liu, F.; Zhang, H. Oxidation-resistant MXene-based melamine foam with ultralow-percolation thresholds for electromagnetic-infrared compatible shielding. *ACS Appl. Mater. Interfaces.* **2022**, *14*, 40396.
(47) Hu, J.; Liang, C.; Li, J.; Lin, C.; Liang, Y.; Dong, D. Ultrastrong and hydrophobic sandwich-structured MXene-based composite films for high-efficiency electromagnetic interference shielding. *ACS Appl. Mater. Interfaces.* **2022**, *14*, 33817.
(48) Yang, Y.; Li, B.; Wu, N.; Liu, W.; Zhao, S.; Zhang, C. J.; Liu, J.; Zeng, Z. Biomimetic porous MXene-based hydrogel for high-performance and multifunctional electromagnetic interference shielding. *ACS Mater. Lett.* **2022**, *4*, 2352.
(49) Chen, Q.; Zhang, K.; Huang, L.; Li, Y.; Yuan, Y. Reduced graphene oxide/MXene composite foam with multilayer structure for electromagnetic interference shielding and heat insulation applications. *Adv. Eng. Mater.* **2022**, *24*, No. 2200098.
(50) Tang, X.; Luo, J.; Hu, Z.; Lu, S.; Liu, X.; Li, S.; Zhao, X.; Zhang, Z.; Lan, Q.; Ma, P.; Wang, Z.; Liu, T. Ultrathin, flexible, and oxidation-resistant MXene/graphene porous films for efficient electromagnetic interference shielding. *Nano Res.* **2023**, *16*, 1755.
(51) Zheng, X.; Tang, J.; Wang, P.; Wang, Z.; Zou, L.; Li, C. Interfused core-shell heterogeneous graphene/MXene fiber aerogel for high-performance and durable electromagnetic interference shielding. *J. Colloid Interface Sci.* **2022**, *628*, 994.
(52) Li, J.; Liang, C.; Hu, J.; Lin, C.; Liang, Y.; Dong, D. Construction of strong and superhydrophobic MXene composite films by binary organosilane cross-linking for electromagnetic interference shielding and joule heating. *Carbon* **2024**, *216*, No. 118567.
(53) Li, S.; Xu, S.; Pan, K.; Du, J.; Qiu, J. Ultra-thin broadband terahertz absorption and electromagnetic shielding properties of MXene/rGO composite film. *Carbon* **2022**, *194*, 127.
(54) Chen, Z. B.; Yang, S. D.; Huang, J. H.; Gu, Y. F.; Huang, W. B.; Liu, S. Y.; Gui, X. C. Flexible, transparent and conductive metal mesh films with ultra-high FoM for stretchable hheating and electromagnetic interference shielding. *Nano-micro Lett.* **2024**, *16*, No. 92.
(55) Jin, L.; Wang, J.; Wu, F.; Yin, Y.; Zhang, B. MXene@Fe_3O_4 microspheres/fibers composite microwave absorbing materials: optimum composition and performance evaluation. *Carbon* **2021**, *182*, 770.
(56) Swapnalin, J.; Koneru, B.; Banerjee, P.; Natarajan, S.; Franco, A. Multilayer intercalation: MXene/cobalt ferrite electromagnetic wave absorbing two-dimensional materials. *J. Phys. Chem. Solids* **2022**, *168*, No. 110797.
(57) Mudasar, M.; Xu, Z. H.; Lian, S. Y.; Li, X.; Wang, J.; Cheng, X. Featuring heterogeneous composite of W-type hexagonal ferrite with 2D vanadium carbide MXene for wideband microwave absorption. *J. Mater. Res. Technol.* **2024**, *28*, 2699.
(58) Wang, Z.; Cheng, Z.; Xie, L.; Hou, X.; Fang, C. Flexible and lightweight $Ti_3C_2T_x$ MXene/Fe_3O_4@PANI composite films for high-performance electromagnetic interference shielding. *Ceram. Int.* **2021**, *47*, 5747.
(59) Won, H.; Hong, Y. K.; Choi, M.; Garcia, H.; Shin, D.; Yoon, Y. S.; Lee, K.; Xin, H.; Yeo, C. D. Microwave absorption performance of M-type hexagonal ferrite and MXene composite in Ka and V bands (5G mmwave frequency bands). *J. Magn. Magn. Mater.* **2022**, *560*, No. 169523.
(60) Guo, H.; Wang, X.; Pan, F.; Shi, Y.; Jiang, H.; Cai, L.; Lu, W.; et al. State of the art recent advances and perspectives in 2D MXene-based microwave absorbing materials: a review. *Nano Res.* **2023**, *16*, 10287−10325.

https://doi.org/10.1021/acsami.4c11189
ACS Appl. Mater. Interfaces XXXX, XXX, XXX−XXX

(61) Zhang, S. L.; Ying, H. J.; Yuan, B.; Hu, R. Z.; Han, W. Q. Partial atomic tin nanocomplex pillared few-layered $Ti_3C_2T_x$ MXenes for superior lithium-ion storage. *Nano-Micro Lett.* **2020**, *12*, 310−313.
(62) Ma, Z.; Feng, H.; Feng, Y.; Ding, X.; Wang, X.; Wang, W.; Li, Q.; et al. An ultralight and thermally conductive $Ti_3C_2T_x$ MXene−silver nanowire cellular composite film for high-performance electromagnetic interference shielding. *J. Mater. Chem. C* **2022**, *10*, 14169−14179.
(63) Zhao, R. Z.; Elzatahry, A.; Chao, D. L.; Zhao, D. Y. Making MXenes more energetic in aqueous batter. *Matter* **2022**, *5*, 8−10.
(64) Wan, B. L.; Liu, N. N.; Zhang, Z.; Fang, X.; Ding, Y. G.; Xiang, H. S.; He, Y. Q.; Liu, M. X.; Lin, X. M.; Tang, J. T.; Li, Y. Z.; Tang, B.; Zhou, G. F. Water-dispersible and stable polydopamine coated cellulose nanocrystal-MXene composites for high transparent, adhesive and conductive hydrogels. *Carbohydr. Polym.* **2023**, *314*, No. 120929.
(65) Xing, Y.; Wan, Y.; Wu, Z.; Wang, J.; Jiao, S.; Liu, L. Multilayer ultrathin MXene@AgNW@MoS_2 composite film for high-efficiency electromagnetic shielding. *ACS Appl. Mater. Interfaces.* **2023**, *15*, 5787.
(66) Wang, W.; Bing, X.; Zhou, Y.; Geng, M.; Zhan, Y.; Xia, H.; Chen, Z. Tunable electromagnetic interference shielding ability of MXene/chitosan/silver nanowire sandwich films. *Funct. Mater. Lett.* **2021**, *14*, No. 2151041.
(67) Yang, S.; Yan, D. X.; Li, Y.; Lei, J.; Li, Z. M. Flexible poly(vinylidene fluoride)-MXene/silver nanowire electromagnetic shielding films with joule heating performance. *Ind. Eng. Chem. Res.* **2021**, *60*, 9824.
(68) Qu, Y.; Li, X.; Wang, X.; Dai, H. Multifunctional AgNWs@MXene/AgNFs electromagnetic shielding composites for flexible and highly integrated advanced electronics. *Compos. Sci. Technol.* **2022**, *230*, No. 109753.
(69) Chang, G.; Zeng, L.; Xie, L.; Xue, B.; Zheng, Q. Ultrathin multifunctional electromagnetic interference shielding MXene/AgNWs/PEDOT:PSS coatings with superior electro/photo-thermal transition ability and water repellency. *Chem. Eng. J.* **2023**, *470*, No. 144033.
(70) Cheng, M.; Ying, M.; Zhao, R.; Ji, L.; Li, H.; Liu, X.; Zhang, J.; Li, Y.; Dong, X.; Zhang, X. Transparent and flexible electromagnetic interference shielding materials by constructing sandwich AgNW@MXene/wood composites. *ACS Nano* **2022**, *16*, 16996.
(71) Liu, L. X.; Chen, W.; Zhang, H. B.; Zhang, Y.; Tang, P.; Li, D.; Deng, Z.; Ye, L.; Yu, Z. Z. Tough and electrically conductive $Ti_3C_2T_x$ MXene−based core−shell fibers for high−performance electromagnetic interference shielding and heating application. *Chem. Eng. J.* **2022**, *430*, No. 133074.
(72) Ma, M.; Tao, W.; Liao, X.; Chen, S.; Shi, Y.; He, H.; Wang, X. Cellulose nanofiber/MXene/FeCo composites with gradient structure for highly absorbed electromagnetic interference shielding. *Chem. Eng. J.* **2023**, *452*, No. 139471.
(73) Rajavel, K.; Hu, Y.; Zhu, P.; Sun, R.; Wong, C. MXene/metal oxides-Ag ternary nanostructures for electromagnetic interference shielding. *Chem. Eng. J.* **2020**, *399*, No. 125791.
(74) Yang, K.; Cui, Y.; Wan, L.; Wng, Y.; Tariq, M. R.; Liu, P.; Zhang, Q.; Zhang, B. Preparation of three-dimensional Mo_2C/NC@MXene and its efficient electromagnetic absorption properties. *ACS Appl. Mater. Interfaces.* **2022**, *14*, 7109.
(75) Duan, N.; Shi, Z.; Wang, Z.; Zou, B.; Zhang, C.; Wang, J.; Xi, J.; Zhang, X.; Zhang, X.; Wang, G. Mechanically robust $Ti_3C_2T_x$ MXene/carbon fiber fabric/thermoplastic polyurethane composite for efficient electromagnetic interference shielding applications. *Mater. Design* **2022**, *214*, No. 110382.
(76) Li, D. Y.; Liu, L. X.; Wang, Q. W.; Zhang, H. B.; Chen, W.; Yin, G.; Yu, Z. Z. Functional polyaniline/MXene/cotton fabrics with acid/alkali-responsive and tunable electromagnetic interference shielding performances. *ACS Appl. Mater. Interfaces* **2022**, *14*, 12703.
(77) Ma, L.; Hamidinejad, M.; Liang, C.; Zhao, B.; Habibpour, S.; Yu, A.; Filleter, T.; Park, B. C. Enhanced electromagnetic wave absorption performance of polymer/SiC-nanowire/MXene($Ti_3C_2T_x$) composites. *Carbon* **2021**, *179*, 408.
(78) Zhang, H.; Wan, J.; Wu, R.; Chen, Y.; Yu, H.; Shi, S. MXenes for electromagnetic interference shielding: insights from structural design. *Carbon* **2024**, *218*, No. 118716.
(79) Liang, C. B.; Gu, Z. J.; Zhang, Y. L.; Ma, Z. L.; Qiu, H.; Gu, J. W. Structural design strategies of polymer matrix composites for electromagnetic interference shielding: a review. *Nano-Micro Lett.* **2021**, *13*, No. 181.
(80) Cao, H. X.; Neal, N. N.; Pas, S.; Radovic, M.; Lutkenhaus, J. L.; Green, M. J.; Pentzer, E. B. Architecting MXenes in polymer composites. *Prog. Polym. Sci.* **2024**, *153*, No. 101830.
(81) Yang, S. J.; Cao, Y.; He, Y. B.; Lv, W. A review of the use of graphene-based materials in electromagnetic-shielding. *Carbon* **2024**, *226*, No. 19130.
(82) He, Y. F.; Su, Q.; Liu, D. D.; Xia, L.; Huang, X. X.; Lan, D.; Zhong, B.; et al. Surface engineering strategy for MXene to tailor electromagnetic wave absorption performance. *Chem. Eng. J.* **2024**, *491*, No. 152041.
(83) Li, R.; Gao, Q.; Xing, H.; Su, Y.; Zhang, H.; Zeng, D.; Fan, B.; Zhao, B. Lightweight, multifunctional MXene/polymer composites with enhanced electromagnetic wave absorption and high-performance thermal conductivity. *Carbon* **2021**, *183*, 301.
(84) Wang, L.; Qiu, H.; Song, P.; Zhang, Y.; Lu, Y.; Liang, C.; Kong, J.; Chen, L.; Gu, J. 3D $Ti_3C_2T_x$ MXene/C hybrid foam/epoxy nanocomposites with superior electromagnetic interference shielding performances and robust mechanical properties. *Composites, Part A* **2019**, *123*, 293.
(85) Cheng, Y.; Lu, Y.; Xia, M.; Piao, L.; Liu, Q.; Li, M.; Zhou, Y.; Jia, K.; Yang, L.; Wang, D. Flexible and lightweight MXene/silver nanowire/polyurethane composite foam films for highly efficient electromagnetic interference shielding and photothermal conversion. *Compos. Sci. Technol.* **2021**, *215*, No. 109023.
(86) Huang, J.; Wang, T.; Su, Y.; Ding, Y.; Tu, C.; Li, W. Hydrophobic MXene/hydroxyethyl cellulose/silicone resin composites with electromagnetic interference shielding. *Adv. Mater. Interfaces* **2021**, *8*, No. 2100186.
(87) Wang, L.; Song, P.; Lin, C. T.; Kong, J.; Gu, J. 3D shapeable, superior electrically conductive cellulose nanofibers/$Ti_3C_2T_x$ MXene aerogels/epoxy nanocomposites for promising EMI shielding. *Research* **2020**, *2020*, No. 4093732.
(88) Yan, Z.; Ding, Y.; Huang, M.; Li, J.; Han, Q.; Yang, M.; Li, W. MXene/CNTs/aramid aerogels for electromagnetic interference shielding and joule heating. *ACS Appl. Nano Mater.* **2023**, *6*, 6141.
(89) Liu, H. G.; Shao, Y. W.; Wang, Z.; Jiang, L. T.; Mou, B.; Tian, N.; You, C.; Li, Y. Mechanically robust and multifunctional $Ti_3C_2T_x$ MXene composite aerogel for broadband EMI shielding. *Carbon* **2024**, *221*, No. 118948.
(90) Ma, Z.; Zhang, L.; Wang, X.; Xiao, G.; Feng, Y.; Wang, W.; Li, Q.; et al. Anchoring magnetic ZIF-67 on $Ti_3C_2T_x$ MXene to form composite films with high electromagnetic interference shielding performance. *J. Mater. Chem. C* **2023**, *11*, 12057−12067.
(91) Zhu, X.; Qian, X.; Hao, M. Y.; Zhang, Y. G.; Zhang, Z. J.; Li, S. J.; Wu, H. N. High performance electromagnetic wave absorbing material based on 3D flower-liked MXene. *J. Alloys Compd.* **2024**, *989*, No. 174440.
(92) Ling, M. Y.; Ge, F. J.; Wu, F.; Zhang, L.; Zhang, Q. Y.; Zhang, B. L. Effect of crystal transformation on the intrinsic defects and the microwave absorption performance of Mo_2 TiC_2T_x/RGO microspheres. *Small* **2023**, *20*, No. e2306233.
(93) Li, Q.; Chen, L.; Ding, J.; Zhang, J.; Li, X.; Zheng, K.; Zhang, X.; Tian, X. Open-cell phenolic carbon foam and electromagnetic interference shielding properties. *Carbon* **2016**, *104*, 90−105.
(94) Zuo, T.; Xie, C.; Wang, W.; Yu, D. $Ti_3C_2T_x$ MXene-ferroferric oxide/carbon nanotubes/waterborne polyurethane-based asymmetric composite aerogels for absorption-dominated electromagnetic interference shielding. *ACS Appl. Nano Mater.* **2023**, *6*, 4716.
(95) Song, P.; Qiu, H.; Wang, L.; Liu, X.; Zhang, Y.; Zhang, J.; Kong, J.; Gu, J. Honeycomb structural rGO-MXene/epoxy nanocomposites for superior electromagnetic interference shielding performance. *Sustainable Mater. Technol.* **2020**, *24*, No. e00153.

https://doi.org/10.1021/acsami.4c11189
ACS Appl. Mater. Interfaces XXXX, XXX, XXX−XXX

(96) Das, P.; Khoshbakht, M. P.; Ganguly, S.; Tang, X. W.; Wang, B.; Srinivasan, S.; Rajabzadeh, A. R.; Rosenkranz, A. M Xene-based elastomer mimetic stretchable sensors: design, properties, and applications. *Nano-Micro Lett.* **2024**, *16*, No. 135.
(97) Wang, W.; Peng, Z.; Ma, Z.; Zhang, L.; Wang, X.; Xu, Z.; Li, Q.; et al. High-efficiency electromagnetic interference shielding from highly aligned MXene porous composites via controlled directional freezing. *ACS Appl. Mater. Interfaces* **2023**, *15*, 47566−47576.
(98) Wang, Q. Q.; Cao, W. Q.; Cao, M. S. MXenes hierarchical architectures: electromagnetic absorbing, shielding and devices. *2D Mater.* **2024**, *11*, No. 012001.
(99) Zhao, Z.; Shi, B.; Wang, T.; Wang, R.; Chang, Q.; Yun, J.; Zhang, L.; Wu, H. Microscopic and macroscopic structural strategies for enhancing microwave absorption in MXene-based composites. *Carbon* **2023**, *215*, No. 118450.
(100) Zhang, G.; Du, M.; Tan, Z.; Zhao, H.; Yi, L.; Ji, X.; Zhao, L. Structure design and properties of MXene-WPU-Co/C electromagnetic shielding composite films. *Mater. Today Commun.* **2023**, *37*, No. 107536.
(101) Guo, Z.; Ren, P.; Lu, Z.; Hui, K.; Yang, J.; Zhang, Z.; Chen, Z.; Jin, Y.; Ren, F. Multifunctional $CoFe_2O_4$@MXene-AgNWs/cellulose nanofiber composite films with asymmetric layered architecture for high-efficiency electromagnetic interference shielding and remarkable thermal management capability. *ACS Appl. Mater. Interfaces* **2022**, *14*, 41468−41480.
(102) Li, Q.; Yang, W.; Sun, K.; Guo, Y.; Liu, H.; Liu, C.; Shen, C. Superhydrophobic flexible conductive PFDT/CB/MXene@paper for high-efficiency EMI shielding and Joule heating applications. *J. Mater. Chem. C* **2022**, *10*, 14560.
(103) Li, J.; Zhang, W.; Yang, L.; Yin, S. Conductive fabrics based on carbon nanotube/$Ti_3C_2T_x$ MXene/polyaniline/liquid metal quaternary composites with improved performance of EMI shielding and joule heating. *Compos. Commun.* **2023**, *38*, No. 101476.
(104) Zuo, T.; Wang, W.; Yu, D. MXene/Ag@ZnO/WPU/melamine gradient composite foams prepared by a unidirectional evaporation approach for absorption-dominated electromagnetic interference shielding. *J. Alloys Compd.* **2023**, *966*, No. 171644.
(105) Ma, M.; Shao, W.; Chu, Q.; Tao, W.; Chen, S.; Shi, Y.; He, H.; Zhu, Y.; Wang, X. Structural design of asymmetric gradient alternating multilayered CNF/MXene/FeCo@rGO composite film for efficient and enhanced absorbing electromagnetic interference shielding. *J. Mater. Chem. A* **2024**, *12*, 1617.
(106) Zhu, L.; Mo, R.; Yin, C. G.; Guo, W.; Yu, J.; Fan, J. Synergistically constructed electromagnetic network of magnetic particle-decorated carbon nanotubes and MXene for efficient electromagnetic shielding. *ACS Appl. Mater. Interfaces* **2022**, *14*, 56120−56131.
(107) Hou, Y.; Liu, K.; Chen, J.; Wang, B.; He, X.; Li, D.; Wei, S.; Li, B.; Han, Q. Bimetallic MOFs/MXene derived CoNi@C@$Ti_3C_2T_x$/TiO_2 nanocomposites for high-efficiency electromagnetic wave absorption. *Carbon* **2024**, *216*, No. 118587.
(108) Li, G.; Tan, R.; Gao, B.; Zhou, Y.; Zhang, C.; Chen, P.; Wang, X. Hierarchical composite CoFe-K/GC@MnO_2@MXene for excellent electromagnetic wave absorption. *J. Alloys Compd.* **2024**, *979*, No. 173580.
(109) Wang, H.; Chen, K.; Shi, Y.; Zhu, Y.; Jiang, S.; Liu, Y.; Wu, S.; Nie, C.; Fu, L.; Feng, Y.; Song, P. Flame retardant and multifunctional BC/MXene/MSiCnw/FRTPU aerogel composites with superior electromagnetic interference shielding via "consolidating" method. *Chem. Eng. J.* **2023**, *474*, No. 145904.

https://doi.org/10.1021/acsami.4c11189
ACS Appl. Mater. Interfaces XXXX, XXX, XXX−XXX